INVESTIGATION OF SOME TETRAGONALLY DISTORTED COBALT(II) COMPLEXES

By

OSCAR RAMIREZ, JR.

A DISSERTATION PRESENTED TO THE GRADUATE COUNCIL OF
THE UNIVERSITY OF FLORIDA
IN PARTIAL FULFILLMENT OF THE REQUIREMENTS FOR THE
DEGREE OF DOCTOR OF PHILOSOPHY

UNIVERSITY OF FLORIDA

August, 1965

ACKNOWLEDGEMENTS

The author wishes to express his sincere appreciation to Dr. R. C. Stoufer, Chairman of the author's Supervisory Committee, and to the other members of the author's Supervisory Committee. For the patient guidance and encouragement given by Dr. R. C. Stoufer, the author expresses his sincere gratitude.

The author wishes to thank Mr. Harold Fisher for tracing many of the figures in this manuscript, and Mrs. Edwin Johnston who typed this manuscript.

The author gratefully acknowledges the support of the National Aeronautics and Space Administration in the form of a Traineeship for the academic year 1964-1965 and of the National Science Foundation under Grant Number GP 1809 in the form of materials and a Graduate Research Assistantship for the academic year 1963-1964.

TABLE OF CONTENTS

LIST OF TABLES

LIST OF FIGURES

Figure Page

INTRODUCTION

In general, six-coordinate compounds of cobalt(II) exhibit high-spin magnetic moments (4.3-5.2 B.M.) (27). There are, in contrast, few examples of six-coordinate complexes exhibiting low-spin magnetic moments (1.8-2.0 B.M.) (15,27). However, compounds such as bis(2,6-pyridindialdihydrazone)cobalt(II) iodide, 2.9 B.M., exhibit magnetic moments which are too small for high-spin complexes and too large for low-spin complexes. Complexes exhibiting these intermediate moments are believed to be near the cross-over between high-spin ($^4T_{1g}$) and low-spin (^2E_g) states (14,17,44).

The characterization of the transition between low- and high-spin states is one of the many intriguing problems yet to be solved in the area of transition metal chemistry. Few relevant examples exist and little is known of the actual transition between these states. Recently, several cobalt(II) compounds reported to exhibit unusual magnetic behavior, have been discussed in terms of an equilibrium mixture of several states characterized by different spin-multiplicities (14,17,44). In most of these examples, the ligands forming these complexes contain the dimethine linkage, -N=C-C=N- .

It has been demonstrated that ligands containing the dimethine linkage produce very large ligand field splittings in their six-coordinate cobalt(II) compounds (ca. 14,000 cm^{-1}) (17,39); nonetheless, Griffith has estimated the pairing energy for cobalt(II) in an octahedral environment to be 22,000 cm^{-1} (20). Liehr has estimated a value of 16,300 cm^{-1} (28); and Ballhausen has estimated a minimum value of 15,400 cm^{-1}; however there appears to be an error in his calculation. Correcting his calculation gives a minimum value of 17,500 cm^{-1} (2). Because these ligands produce splittings considerably lower than the pairing energy quoted by the above authors, it has been suggested that a tetragonal distortion of some of these complexes may be the factor causing pairing of electrons.

The assertion that a tetragonal distortion will facilitate spin-pairing in these complexes is based on the following crude extrapolations and observations (45).

A compression (increase in ligand field strength) along the z-axis of an octahedral complex (Figure 1) will increase the energies of the d_{z^2}, d_{xz}, and d_{yz} orbitals; however, the energy of the d_{z^2} orbital will be increased to a greater extent than that of the latter two. To a first approximation, the energies of the $d_{x^2-y^2}$ and d_{xy} orbitals will remain the same as in the regular octahedral environment. It can easily be seen that the energy separation (Δ') which

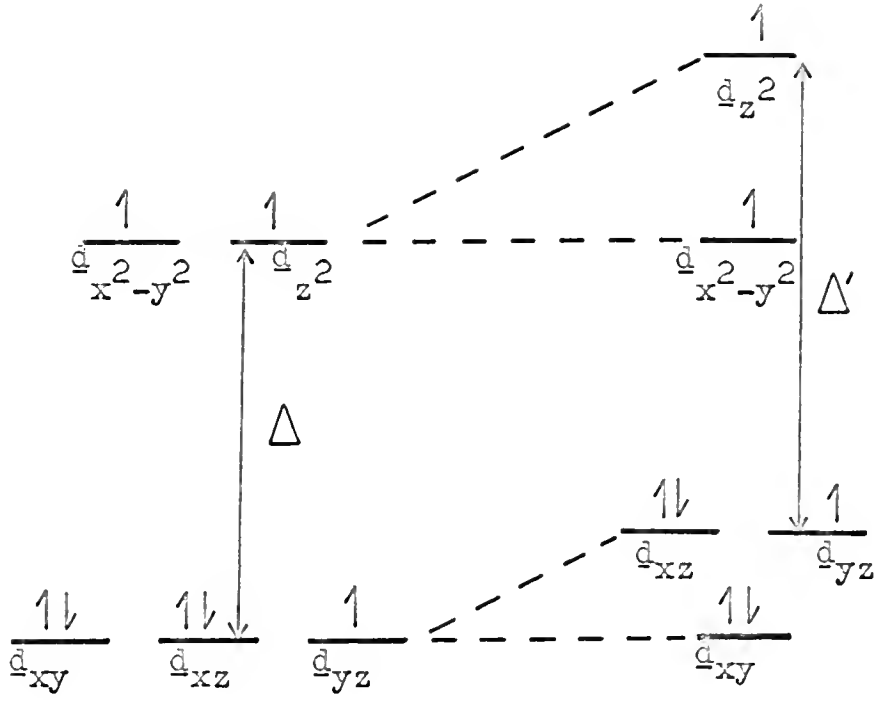

Fig. 1.-d-Orbital energy level diagram in an octahedral field and in an axially compressed field.

determines whether or not spin-pairing will occur in the distorted complex is larger than that in the regular octahedral complex.

An extension along the z-axis of an octahedral complex produces, in the limit, a planar complex. Because planar complexes of cobalt(II) containing unsaturated nitrogen donor atoms are low-spin (2.1-2.9 B.M.), one would expect a tetragonal distortion to favor pairing of electrons.

The purpose of the investigations reported in this dissertation was to test the above postulates by preparing and characterizing a series of six-coordinate cobalt(II) complexes in which the magnitude of a tetragonal component is varied. The complexes are of the type, CoX_2L_2 and CoX_2L', where X is a monodentate ligand, L is 2-pyridinal-p-tolylimine (PAT)* (Structure I), and L' is bis(2-pyridinal)-o-phenylenediimine (PAPI)* (Structure II). Several other metal complexes containing these ligands have been prepared in order to facilitate the characterization of the analogous cobalt(II) complexes.

---

*These abbreviations will be used throughout this dissertation.

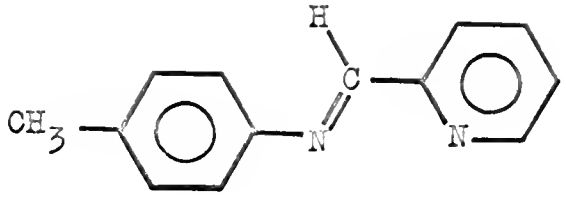

Structure I

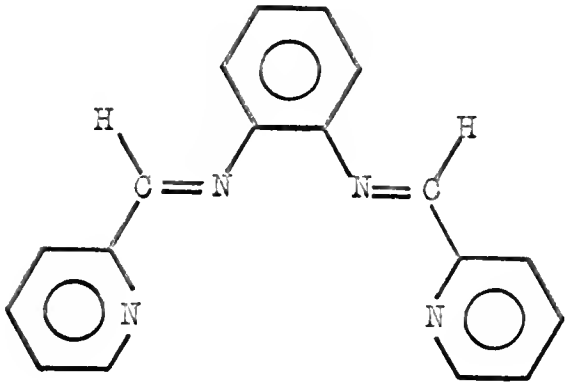

Structure II

EXPERIMENTAL PROCEDURES

2-Pyridinal-p-tolylimine, PAT.--This ligand was prepared essentially in the manner given by G. Bahr and H. Thamlitz (1) except that the product was not fractionally distilled but merely recrystallized from hexane; m.p. 57-58°C.

Dichlorobis(2-pyridinal-p-tolylimine)cobalt(II), $[CoCl_2(PAT)_2]$.--A solution of 2-pyridinal-p-tolylimine (3.72 g, 0.019 mole) in absolute ethanol (approximately 25 ml) was added slowly with constant agitation to a solution of cobalt(II) chloride hexahydrate (2.38 g, 0.01 mole) in absolute ethanol (approximately 25 ml). The orange-red microcrystalline product which formed when placed on an ice-bath was collected on a sintered glass filter under an abundant flow of nitrogen, washed with a few ml of cold absolute ethanol, and dried over P_4O_{10} *in vacuo* at 95°C for five hours.

Anal. Calcd. for $CoC_{26}H_{24}N_4Cl_2$: C, 59.79; H, 4.63; N, 10.73. Found: C, 59.49; H, 4.52; N, 10.46. Yield 7.0 g.

Dibromobis(2-pyridinal-p-tolylimine)cobalt(II), $[CoBr_2(PAT)_2]$.--A solution of 2-pyridinal-p-tolylimine

(7.84 g, 0.04 mole) in absolute ethanol (approximately 25 ml) was added slowly with constant agitation to a solution of cobalt(II) bromide (4.38 g, 0.02 mole) in absolute ethanol (approximately 18 ml). The orange-red product crystallized from the solution at room temperature, was collected on a sintered glass filter under an abundant flow of nitrogen, washed with a few ml of cold absolute ethanol, and dried over P_4O_{10} *in vacuo* at room temperature.

Anal. Calcd. for $CoC_{26}H_{24}N_4Br_2$: C, 51.09; H, 3.96; N, 9.17. Found: C, 51.18; H, 4.05; N, 9.19. Yield 11.3 g.

Diiodobis(2-pyridinal-p-tolylimine)cobalt(II), $[CoI_2(PAT)_2]$.--This product was prepared by a method analogous to that used for $[CoBr_2(PAT)_2]$, except that anhydrous cobalt(II) iodide was used. A gummy material formed when the solution was placed on an ice-bath. Upon addition of excess concentrated aqueous potassium iodide solution with stirring, the gum slowly crystallized. The orange product was collected on a sintered glass filter under an abundant flow of nitrogen, washed with several portions of distilled water, and dried over P_4O_{10} *in vacuo* at 90°C for about five hours.

Anal. Calcd. for $CoC_{26}H_{24}N_4I_2$: C, 44.28; H, 3.43; N, 7.94. Found: C, 43.95; H, 3.60; N, 7.81. Yield 8.3 g.

Dinitritobis(2-pyridinal-p-tolylimine)cobalt(II), $[Co(NO_2)_2(PAT)_2]$.--A solution of 2-pyridinal-p-tolylimine (7.84 g, 0.04 mole) in water was added slowly with constant agitation to a solution of cobalt(II) chloride hexahydrate (4.76 g, 0.02 mole) in water. A gummy material was formed upon the addition of a solution of sodium nitrite (2.76 g, 0.04 mole) in water. Excess sodium nitrite solution was added to the mixture with agitation. The gum slowly crystallized. The orange product was collected and washed with several portions of distilled water, and dried over P_4O_{10} *in vacuo* at 100°C for six hours.

Anal. Calcd. for $CoC_{26}H_{24}N_6O_4$: C, 57.45; H, 4.45; N, 15.47. Found: C, 57.21; H, 4.51; N, 15.21. Yield 7.7 g.

Diisothiocyanatobis(2-pyridinal-p-tolylimine)-cobalt(II), $[Co(NCS)_2(PAT)_2]$.--This product was prepared by a method analogous to that used for $[Co(NO_2)_2(PAT)]$ except that absolute ethanol was used as the solvent and potassium thiocyanate was used in excess. A gummy material was formed which eventually crystallized. The product was filtered, dissolved in dimethyl formamide, refiltered, then recrystallized by reducing the volume of the solution. The orange product was collected, washed with absolute ethanol, and dried over P_4O_{10} *in vacuo* at room temperature.

Anal. for $CoC_{28}H_{24}N_6S_2$: C, 59.25; H, 4.26; N, 14.81. Found: C, 59.14; H, 4.24; N, 14.55. This complex can be

made more easily by using anhydrous cobalt thiocyanate and following the procedure used for [$CoBr_2$(PAT)]. Yield 5.7 g.

Dichloro[bis(2-pyridinal)-o-phenylenediimine]-cobalt(II), [$CoCl_2$(PAPI)].--Five ml (0.053 mole) of 2-pyridinecarboxaldehyde was added slowly and with constant stirring under an abundant flow of nitrogen to a solution (2.60 g, 0.02 mole) of anhydrous cobalt(II) chloride in absolute ethanol (40 ml). To this solution was added a solution of freshly sublimed o-phenylenediamine (2.16 g, 0.02 mole) in absolute ethanol (25 ml) with constant stirring and under nitrogen. On continued stirring a butterscotch-colored product formed, which was collected on a sintered glass filter under nitrogen, washed thoroughly with absolute ethanol, and dried first at room temperature over P_4O_{10} *in vacuo*, then at 100°C for six hours. The use of nitrogen was a precautionary measure because these complexes appear quite stable to oxidation in air.

Anal. Calcd. for $CoC_{14}H_{18}N_4Cl_2$: C, 51.95; H, 3.39; N, 13.46. Found: C, 51.90; H, 3.50; N, 13.29. Yield 6.4 g.

Dibromo[bis(2-pyridinal)-o-phenylenediimine]-cobalt(II), [$CoBr_2$(PAPI)].--This rich brown product was prepared by a method analogous to that used for [$CoCl_2$(PAPI)] except that anhydrous cobalt(II) bromide was used.

Anal. Calcd. for $CoC_{14}H_{18}N_4Br_2$: C, 42.80; H, 2.79; N, 11.09. Found: C, 42.90; H, 2.93; N, 11.19. Yield 7.3 g.

Diiodo[bis(2-pyridinal)-o-phenylenediimine]cobalt(II), $[CoI_2(PAPI)]$.--This rust-colored product was prepared by a method analogous to that used for $[CoCl_2(PAPI)]$ except that anhydrous cobalt(II) iodide was used.

Anal. Calcd. for $CoC_{14}H_{18}N_4I_2$: C, 36.09; H, 2.36; N, 9.34. Found: C, 36.27; H, 2.54; N, 9.15. Yield 9.1 g.

Diisothiocyanato[bis(2-pyridinal)-o-phenylenediimine]cobalt(II), $[Co(NCS)_2(PAPI)]$.--This straw-colored product was prepared by a method analogous to that used for $[CoCl_2(PAPI)]$ except that anhydrous cobalt(II) thiocyanate was used.

Anal. Calcd. for $CoC_{16}H_{18}N_6S_2$: C, 52.06; H, 3.06; N, 18.21. Found: C, 52.21; H, 3.20; N, 18.14. Yield 5.4 g.

Diperchlorato[bis(2-pyridinal)-o-phenylenediimine]-cobalt(II), $[Co(ClO_4)_2(PAPI)]$.--This dark maroon product was prepared by a method analogous to that used for $[CoCl_2(PAPI)]$ except that cobalt(II) perchlorate hexahydrate was used.

Anal. Calcd. for $CoC_{14}H_{18}N_4Cl_2O_8$: C, 39.73; H, 2.59; N, 10.30. Found: C, 40.08; H, 2.70; N, 10.27. Yield 9.0 g.

Dinitro[bis(2-pyridinal)-o-phenylenediimine]-cobalt(II), $[Co(NO_2)_2(PAPI)]$.--Three grams (0.044 mole) of sodium nitrite were added to a solution (4.76 g, 0.02 mole) of cobalt(II) chloride hexahydrate in a 3:1 ethanol:water mixture (25 ml). All the sodium nitrite did not dissolve but was kept in suspension by constant stirring. Five ml (0.053 mole) of 2-pyridinecarboxaldehyde was added slowly under an abundant flow of nitrogen and with constant stirring to the above solution. To the resulting solution was added slowly a solution of recrystallized (from chloroform) o-phenylenediamine (2.16 g, 0.02 mole) in 3:1 ethanol:water mixture (25 ml) with constant stirring under nitrogen. On continued stirring a rust-colored product formed, which was collected on a sintered glass filter under nitrogen, washed once with 3:1 ethanol:water mixture, followed by a thorough washing with 95 per cent ethanol, then with absolute ethanol, and dried first at room temperature over P_4O_{10} *in vacuo*, then at 100°C for six hours.

Anal. Calcd. for $CoC_{14}H_{18}N_6O_4$: C, 49.44; H, 3.23; N, 19.22. Found: C, 49.33; H, 3.35; N, 19.20. Yield 3.0 g.

Green dichloro[bis(2-pyridinal)-o-phenylenediimine]-cobalt(II), $CoCl_2(PAPI)$.--This green product was prepared in a manner analogous to that used by Petrofsky (37). Four ml (0.042 mole) of 2-pyridinecarboxaldehyde was added to a

solution (2.16 g, 0.02 mole) of freshly sublimed o-phenylenediamine in absolute ethanol (25 ml) and the mixture was refluxed for twenty minutes. To this previously cooled solution was added a solution (4.76 g, 0.02 mole) of cobalt(II) chloride hexahydrate in absolute ethanol (25 ml) with stirring and under a flow of nitrogen. A dark green gummy material was immediately formed which crystallized on continued stirring. The product was collected on a sintered glass filter under nitrogen, washed thoroughly with absolute ethanol, and dried at 90°C over P_4O_{10} *in vacuo* for six hours.

Anal. Calcd. for $CoC_{14}H_{18}N_4Cl_2 \cdot H_2O$: C, 49.73; H, 3.71; N, 12.89. Found: C, 49.63; H, 3.90; N, 12.72. Yield 4.2 g.

Green dibromo[bis(2-pyridinal)-o-phenylenediimine]-cobalt(II), $CoBr_2$(PAPI).--This green material was prepared in a manner analogous to that used for the green $CoCl_2$(PAPI) except that anhydrous cobalt(II) bromide was used.

Anal. Calcd. for $CoC_{14}H_{18}N_4Br_2$: C, 42.80; H, 2.79; N, 11.09. Found: C, 42.55; H, 2.99; N, 10.86. Yield 5.9 g.

Dichloro[bis(2-pyridinal)-o-phenylenediimine]nickel-(II) sesquihydrate, $[NiCl_2(PAPI)] \cdot 3/2\ H_2O$.--This mustard-colored product was prepared in a manner analogous to that used for $[CoCl_2(PAPI)]$ except that nickel(II) chloride hexahydrate was used.

Anal. Calcd. for $NiC_{14}H_{18}N_4Cl_2$ 3/2 H_2O: C, 48.80; H, 3.87; N, 12.65. Found: C, 49.09; H, 4.00; N, 12.56. Yield 5.0 g. After heating to 190°C in vacuo over P_4O_{10} found: N, 12.81.

Dibromo[bis(2-pyridinal)-o-phenylenediimine]nickel-(II) sesquihydrate, $[NiBr_2(PAPI)]\cdot 3/2\ H_2O$.--This tan product was prepared in a manner analogous to that used for $[CoCl_2(PAPI)]$ except that anhydrous nickel(II) bromide was used.

Anal. Calcd. for $NiC_{14}H_{18}N_4Br_2$ 3/2 H_2O: C, 40.65; H, 3.20; N, 10.53. Found: C, 40.78; H, 3.40; N, 10.25. Yield 6.1 g.

Diiodo[bis(2-pyridinal)-o-phenylenediimine]nickel(II), $[NiI_2(PAPI)]$.--This orange product was prepared in a manner analogous to that used for $[Co(NO_2)_2(PAPI)]$ except that nickel(II) chloride hexahydrate and potassium iodide were used.

Anal. Calcd. for $NiC_{14}H_{18}N_4I_2$: C, 36.10; H, 2.36; N, 9.36. Found: C, 35.89; H, 2.57; N, 9.45. Yield 9.7 g.

Aquo-2-pyridinal[bis(2-pyridinal)-o-phenylenediimine]-nickel(II) perchlorate, $[Ni(H_2O)(PA)(PAPI)](ClO_4)_2$.--This rose-beige product was prepared in a manner analogous to that used for $[CoCl_2(PAPI)]$ except that nickel(II) perchlorate hexahydrate was used.

Anal. Calcd. for $NiC_{14}H_{18}N_4I_2$: C, 36.10; H, 2.36; N, 9.36. Found: C, 35.89; H, 2.57; N, 9.45. Yield 9.7 g.

Aquo-2-pyridinal[bis(2-pyridinal)-o-phenylenediimine]nickel(II) perchlorate, $[Ni(H_2O)(PA)(PAPI)](ClO_4)_2$.--This rose-beige product was prepared in a manner analogous to that used for $[CoCl_2(PAPI)]$ except that nickel(II) perchlorate hexahydrate was used.

Anal. Calcd. for $NiC_{20}H_{21}N_5O_8Cl_2$: C, 43.08; H, 3.16; N, 10.47. Found: C, 42.96; H, 3.29; N, 10.58. Yield 9.8 g.

All analytical measurements were made by Galbraith Microanalytical Laboratories, Knoxville, Tennessee.

Apparatus

Magnet. The magnetic susceptibilities were determined by the Gouy method. The equipment has been described previously (8). The magnet used was a Varian Associates Model V-4004 equipped with 4 inch cylindrical pole pieces, separated by an air gap of 2-1/4 inches. A Varian Associates Model V-2300-A power supply and a Varian Associates Model V-2301-A current regulator were used to provide a current constant to within $\pm$ 1 x 10^{-3} amp. The maximum field strength attained was 6860 gauss. The magnetic field was calibrated by using water, solid nickel ammonium sulfate hexahydrate, and tris(ethylenediamine)nickel(II) thiosulfate (13).

Cryostat and temperature control. The cryostat and temperature control apparatus used were of the basic design of Figgis and Nyholm (16). Temperatures between 100 and 400°K could be controlled with less than 0.1 degree fluctuation (8).

Sample tube. A quartz sample tube, approximately 3.5 mm inside diameter and approximately 19.0 cm in length, was suspended in the cryostat from a semi-micro balance by a diamagnetic gold chain attached to the tapered Teflon plug. The diamagnetic correction of the tube was measured as a function of the temperature between 100 and 400°K.

Balance. A Mettler Model B-6 semi-micro balance of 0.01 mg sensitivity was used to measure the force exerted by the magnetic field upon the sample.

Spectrometers. A Cary Model 14 Recording Spectrometer was used to determine the ultraviolet, visible, and near infrared spectra of the complexes. The solid state spectra were obtained by using a Cary Model 1411 Diffuse Reflectance Accessory. Magnesium carbonate was used as the reference. A Perkin-Elmer Corporation Model 137B Infracord recording spectrometer was used to determine the infrared spectra of the complexes.

Conductance apparatus. All conductances were measured using an Industrial Instruments, Inc., Model RCM

15 B1 Serfass conductivity bridge and a cell with a constant of 1.485 cm^{-1}. All measurements were made at 25°C in absolute ethanol, using 10^{-3} M solutions. A silicone oil bath, regulated by a Sargent Thermonitor, Model SW, was used to maintain constant temperature. The absolute ethanol had a conductance of less than 5×10^{-7} mho cm^{-1}.

X-ray diffraction apparatus. The x-ray diffraction patterns were obtained by use of a Phillips Electronic Instruments Recording Diffractometer equipped with a copper target. A single crystal monochromator was used to reduce fluorescent background.

RESULTS AND DISCUSSION

Conductance measurements

The specific conductances of the PAT complexes and of the green $CoBr_2$(PAPI) complex in absolute ethanol were measured at 25°C. The values obtained are reported in Table 1. There was no apparent change in color upon solution of these complexes. The specific conductances of the octahedral PAPI complexes (*vide infra*) were not measured because each of these complexes undergoes a pronounced color change upon solution in the few solvents in which appreciable solubility was exhibited. The absolute ethanol used in these determinations had a specific conductance of less than 5×10^{-7} mho cm^{-1}.

The complexes reported in this investigation have been formulated either as four- or six-coordinate species. Numerous examples of each type exist. Six-coordinate complexes, under ideal conditions, should behave as non-electrolytes, that is, the two uni-negative anions should occupy the fifth and sixth coordination sites. However, the observed conductances fall slightly below those characteristic of a uni-univalent electrolyte. For instance, tetraethylammonium bromide has a specific conduc-

TABLE 1

SPECIFIC CONDUCTANCES AT 25.0°C

Complex	Specific conductance (10^{-3}M) micromho/cm
$[CoCl_2(PAT)_2]$	31.7
$[CoBr_2(PAT)_2]$	30.5
$[CoI_2(PAT)_2]$	36.8
$[Co(NO_2)_2(PAT)_2]$	23.2
$[Co(NCS)_2(PAT)_2]$	----
$CoCl_2$(PAPI) green	27.0*
$CoBr_2$(PAPI) green	32.2

*Value reported by Petrofsky (37).

tance in absolute ethanol of 44.0 μmho cm^{-1} in a 1 x 10^{-3} molar solution, a value which falls within the range (40-50 μmho cm^{-1}) of specific conductances quoted for other uni-univalent electrolytes in absolute ethanol (29).

The observed conductances of these complexes might be explained on the basis of an ionic five-coordinate complex; however, there is no compelling reason to formulate such an unusual coordination number for cobalt(II). Rather, cobalt(II) is so labile, that it seems more reasonable to assume that these complexes are six-coordinate in the solid state and that upon solution they undergo partial anion displacement by the solvent molecules. These conductances are not unique to ethanolic solutions of these complexes. Indeed, similar observations have been reported for related complexes in methanol (38) and in N,N-dimethylformamide (37) and rationalized on the basis of anion displacement by the solvent. Furthermore, infrared data substantiate (see Vibrational Spectra) coordination of the weakest coordinating anion, perchlorate, in the solid state. Certainly it is reasonable to expect the stronger bases, viz., Cl^-, Br^-, NO_2^-, etc., to be coordinated also to the metal ion in the solid state.

Vibrational spectra

The infrared spectrum provides another useful tool in the characterization of inorganic complexes. In this

investigation, differentiation between linkage isomers and between ionic and coordinated anions was made possible by using this technique.

The major portion of the spectra of the complexes can be assigned to the constituent groups of the organic ligand (see Appendix I). The infrared spectra of the two PAPI series differ. This observation is expected because in the green PAPI complexes the organic ligand is presumed to be non-planar, acting either as a bi- or tridentate ligand, whereas in the other series it is planar, serving as a tetradentate ligand. Thus, the appearance or absence of some bands in the spectra of the two series is expected on the basis of symmetry differences; some bands become allowed as others become forbidden, etc. Interactions between groups in the different conformations would also cause differences in the spectra.

The complexes within a series containing halogen anions exhibit the same characteristic spectrum not only because the metal-halogen bond stretching vibrations do not appear in the region which was studied, but also because these complexes have similar structures and organic ligand bond energies. On the other hand, the complexes containing polyatomic anions are characterized by the vibrational spectra of the anions superimposed upon the spectrum of the remainder of the complex.

The changes in the infrared spectrum of the perchlorate ion upon coordination have been extensively investigated by Hathaway and Underhill (21). These conclusive investigations have been substantiated by Wickenden and Krause (47).

The uncoordinated perchlorate ion of T_d symmetry has two infrared active vibrational modes (21). One of these occurs as a strong and broad band at approximately 1,110 cm^{-1}. The second band occurs at 630 cm^{-1}, beyond the range studied. The band at 930 cm^{-1} which is infrared forbidden is observed as a very weak absorption (21). The coordinated (through one oxygen atom) perchlorate entity has C_{3v} symmetry. Upon reduction from T_d to C_{3v} symmetry, the broad absorption band present in the ionic perchlorate is split into two well-defined bands with maxima at 1,200 and 1,000 cm^{-1} (21). The originally forbidden infrared absorption now appears as a strong band between 940 and 890 cm^{-1}.

It was found that in $[Ni(H_2O)(PA)(PAPI)](ClO_4)_2$, the perchlorate entity is ionic and exhibits the characteristic broad absorption with a maximum at approximately 1,085 cm^{-1} and the weaker absorption at 930 cm^{-1}. In $[Co(ClO_4)_2(PAPI)]$, however, the perchlorate entity is coordinated and exhibits two strong bands with maxima at 1,110 and 1,035 cm^{-1} and a somewhat weaker band at 920 cm^{-1}. The fact that the perchlorate ion is coordinated in this complex is very important in this investigation (see Magnetic Measurements).

The SCN group may coordinate through either the nitrogen atom or the sulfur atom -- or through both (forming a bridged species). In the first instance the group is referred to as isothiocyanato and in the second, as thiocyanato. Various investigators have studied the effect of linkage isomerization on the C-S stretching frequency (5,6, 7,26,40,46). It is observed that the C-S stretching frequency is shifted to higher wave numbers in the spectra of isothiocyanates and to lower wave numbers in the spectra of thiocyanates, both relative to the C-S stretching frequency of "ionic" KSCN (749 cm^{-1}). Turco and Pecile give the following ranges for the C-S stretching vibration: M-SCN, 690 - 720 cm^{-1}; M-NCS, 780 - 860 cm^{-1} (46). According to Chatt and Duncanson, the C≡N vibration of the group acting as a bridge absorbs near 2182 - 2150 cm^{-1}, whereas this vibration occurs at lower wave numbers in non-bridging groups (7).

The infrared spectrum of $[Co(NCS)_2(PAPI)]$ exhibits a weak absorption at 800 cm^{-1}. There are no absorptions in the 690 - 720 cm^{-1} region. Furthermore, this absorption at 800 cm^{-1} does not appear in the spectra of the other PAPI complexes, so it may be assumed that this is the C-S absorption, thereby indicating that it is the nitrogen atom which is attached to the metal ion. The C≡N absorption appears at about 2090 cm^{-1} indicating that the group is not

bridging. The C≡N absorption appears to be less sensitive to linkage isomerism than is the C-S absorption; however, an extensive tabulation of C≡N absorption maxima reported by Burmeister and Basolo indicate that the majority of C≡N absorptions of isothiocyanates fall slightly below 2100 cm^{-1}; whereas, the C≡N absorption of thiocyanates mainly fall slightly above 2100 cm^{-1} (5).

The spectrum of $[Co(NCS)_2(PAT)_2]$ does not contain a C-S absorption in either characteristic region. There are four absorptions, common to all the PAT complexes, between 830 - 700 cm^{-1} which probably obscure the C-S vibration. The C≡N absorption appears at 2090 cm^{-1} (non-bridging). It is unfortunate that the infrared spectrum could not be more conclusive for this complex; it may still be assumed quite reasonably, however, that the nitrogen atom is attached to the metal ion. In support of this conclusion, Nakamoto states that it is known from x-ray analysis that metals of the first transition series form M-N bonds; whereas those of the second half of the second and third transition series form M-S bonds with the thiocyanate group (33).

The infrared spectrum of $[Co(NO_2)_2(PAPI)]$ is consistent with that of a nitrito complex, that is, coordination of the NO_2 group through oxygen. Nakamoto lists the symmetric stretching vibration of the nitrito group at approximately 1065 cm^{-1} and that of the nitro group at

approximately 1,325 cm^{-1} (33). The absorption maximum of the NO_2 group in the spectrum of the above complex appears at 1,135 cm^{-1}.

The infrared spectrum of $[Co(NO_2)_2(PAT)_2]$ also indicates that the oxygen is coordinated to the metal. The absorption maxima of the symmetric stretching vibration of the nitrito group in the spectrum of this complex appears at 1,070 cm^{-1}.

Electronic spectra

The ultraviolet spectra of the PAT and the green $CoBr_2$(PAPI) complexes in absolute ethanol were recorded. The absorption maxima and corresponding absorptivity coefficients are reported in Table 2.

The very intense absorptions in the region from 2,000 A to 3,500 A are usually due to transitions between the energy levels of the ligand or between the energy levels of the metal ion and the ligand (25,34,35). But, few definite assignments of absorptions by compounds containing complex ligand systems have been made in this region. Unless one has made a detailed study of the energy levels in a complex, assignment of specific transitions is very difficult. Nonetheless, variations in the spectra of similar complexes may often be interpreted in a qualitative manner.

TABLE 2

ULTRAVIOLET ABSORPTIONS

Complex	λ_{max} (A)	$\epsilon \times 10^{-3}$	λ_{max} (A)	$\epsilon \times 10^{-3}$	λ_{max} (A)	$\epsilon \times 10^{-3}$	λ_{max} (A)	$\epsilon \times 10^{-3}$
PAT*	----	----	2390	11.0	----	----	----	----
	----	----	2470	12.0	2900	10.0	3310	8.0
$[Co(PAT)_3]I_2 \cdot 3H_2O$*	2230	25.0	2410	16.0	2860	12.0	3310	9.6
$[CoCl_2(PAT)_2]$	----	----	2375	19.0	2925	15.0	3268	24.0
$[CoBr_2(PAT)_2]$	----	----	2420	13.0	2915	9.5	3300	18.0
$[CoI_2(PAT)_2]$	2175	42.0	----	----	2910	15.0	3260	17.0
$[Co(NO_2)_2(PAT)_2]$	----	----	2385	26.0	2800	18.0	3300	20.0
$[Co(NCS)_2(PAT)_2]$	----***	----	----	----	----	----	----	----
PAPI	2160	15.0	2480	7.1	2550	7.5	2950	17.0

TABLE 2 - Continued

Complex	λ_{max} (A)	$\epsilon \times 10^{-3}$	λ_{max} (A)	$\epsilon \times 10^{-3}$	λ_{max} (A)	$\epsilon \times 10^{-3}$	λ_{max} (A)	$\epsilon \times 10^{-3}$
$CoCl_2$(PAPI)** (green)	----	----	2370	12.0	2600 2600	7.1 7.1	3200	14.0
$CoBr_2$(PAPI) (green)	----	----	2375	12.0	2610 2670	8.0 8.0	3175	14.0

*Values reported by Stoufer (43).

**Values reported by Petrofsky (37).

***Solubility less than 1×10^{-4} M.

The transitions within the ligand usually involve the pi system. The pi system of the ligand may or may not be involved in the formation of bonds with the metal ion upon complexation. If they are not involved, the spectrum of the free ligand will be essentially unchanged upon complexation. On the other hand, if they are involved, the spectrum of the complex may be considerably different from that of the free ligand. This behavior may be a useful criterion for determining the degree of ligand-metal interaction in some of the complexes reported in this investigation.

The ultraviolet spectra of PAT and $[Co(PAT)_3]I_2 \cdot 3H_2O$ have been reported by Stoufer (43). Stoufer found that the spectrum of the tris-complex was essentially the same as that of the free ligand. This behavior was observed also for the bis-complexes of PAT reported in this present investigation. The very intense absorption at 2,175 A in the spectrum of the $[CoI_2(PAT)_2]$ complex is attributable to a charge transfer transition between the iodide ion and the solvent (35). This absorption is so intense that it probably masks the weaker absorption at approximately 2,400 A appearing in the PAT complexes which do not contain iodide ion. Since the spectra of the complexes were found to be essentially the same as that of the free ligand, it may be concluded that the ligand pi system is not involved greatly in bonding with the metal.

Despite repeated attempts by this investigator and by Petrofsky (37), the free PAPI ligand could not be isolated. However, a solution spectrum, presumably of this ligand prepared *in situ* was recorded by Petrofsky (37). The spectra of the two green complexes do differ from that of the free ligand. The absorption at 2,480 A in the free ligand spectrum appears to be shifted to shorter wavelengths in the spectrum of the coordinated ligand; whereas the absorption at 2,950 A is shifted to longer wavelengths. The absorption at 2,550 A is split into two bands, both appearing at slightly longer wavelengths. These shifts and splitting of the absorption maxima may be attributable to pi interaction with the metal, as mentioned above; but in this particular situation this may not be the only reason for a change in the spectrum upon complexation. The free ligand can exist in a number of conformations which are distinct from that of the coordinated ligand. A change in conformation could alter the pi system and, thereby, the ultraviolet spectrum.

A Stuart-Briegleb model of the free ligand shows that there is some interaction between the adjacent hydrogen atoms on the pyridyl and phenyl groups. This interaction tends to force the ligand out of a square planar conformation. It is believed also (*vide infra*) that the cobalt(II) ion in each of the two green PAPI complexes is four coordinate, the ligand assuming a non-planar conformation

and acting as either a bidentate or tridentate ligand. The most stable conformation of the free ligand may well remain the same upon coordination, in which case the change in the ultraviolet spectrum is attributable to participation of the pi system in metal-ligand bonding rather than to a change in conformation. Therefore, further investigation is required before the observed behavior can be explained more definitely.

The diffuse reflectance spectra of the complexes were recorded from 13,500 A to 3,000 A and are shown in Figures 2 through 14. A list of the absorption maxima and shoulders is given in Tables 3, 4, and 5.

The visible spectra of nickel(II) complexes have been interpreted in terms of the ligand field theory by many investigators (4,18,30,31,36,39). The absorption maxima exhibited by the spectra of these complexes usually agree very closely with ligand field predictions. Furthermore, these maxima are better defined than are those for other complexes. For this reason, the spectra of nickel(II) complexes have been very useful in the determination of Δ values for a great variety of ligands. Thus, the nickel(II) complexes reported in this investigation were prepared to obtain an independent evaluation of relative ligand field strengths.

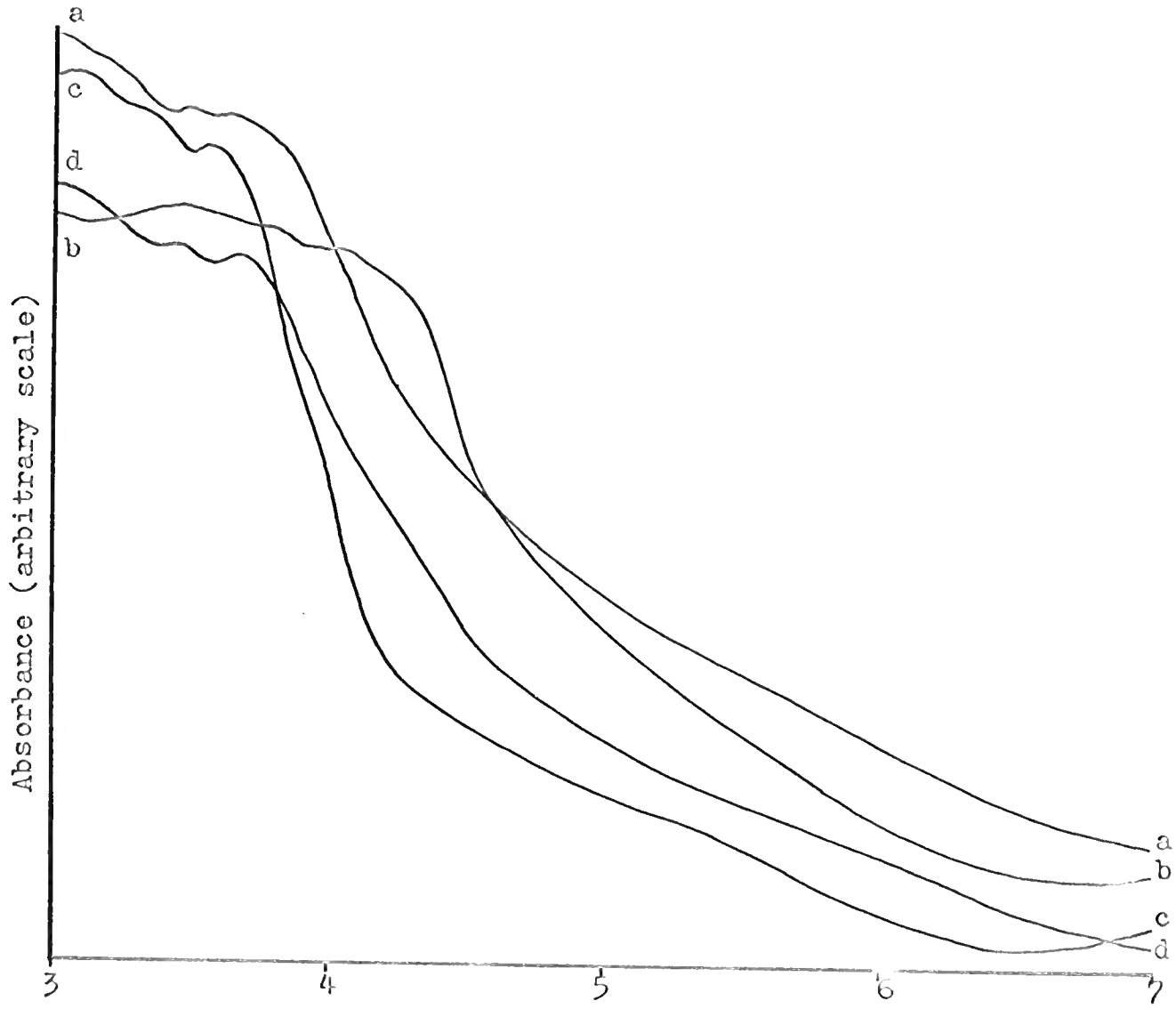

Fig. 2.-Diffuse reflectance spectra of (a) $[NiBr_2(PAPI)]$, (b) $[NiI_2(PAPI)]$, (c) $[Ni(H_2O)(PA)(PAPI)](ClO_4)_2$, and (d) $[NiCl_2(PAPI)]$ from 3,000 to 7,000 A.

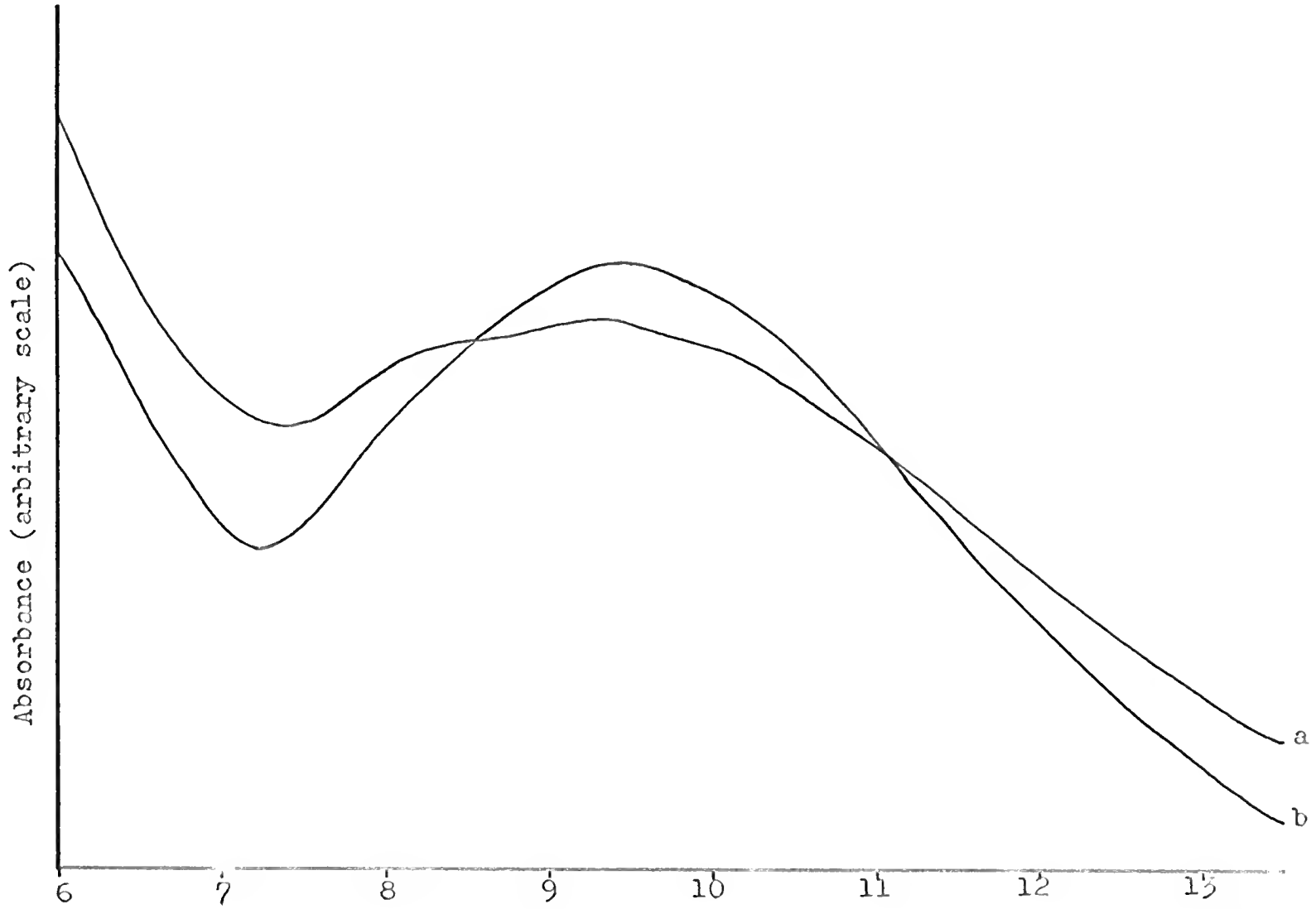

Fig. 3.--Diffuse reflectance spectra of (a) [$NiBr_2$(PAPI)] and (b) [$NiCl_2$(PAPI)] from 6,000 to 13,500 A.

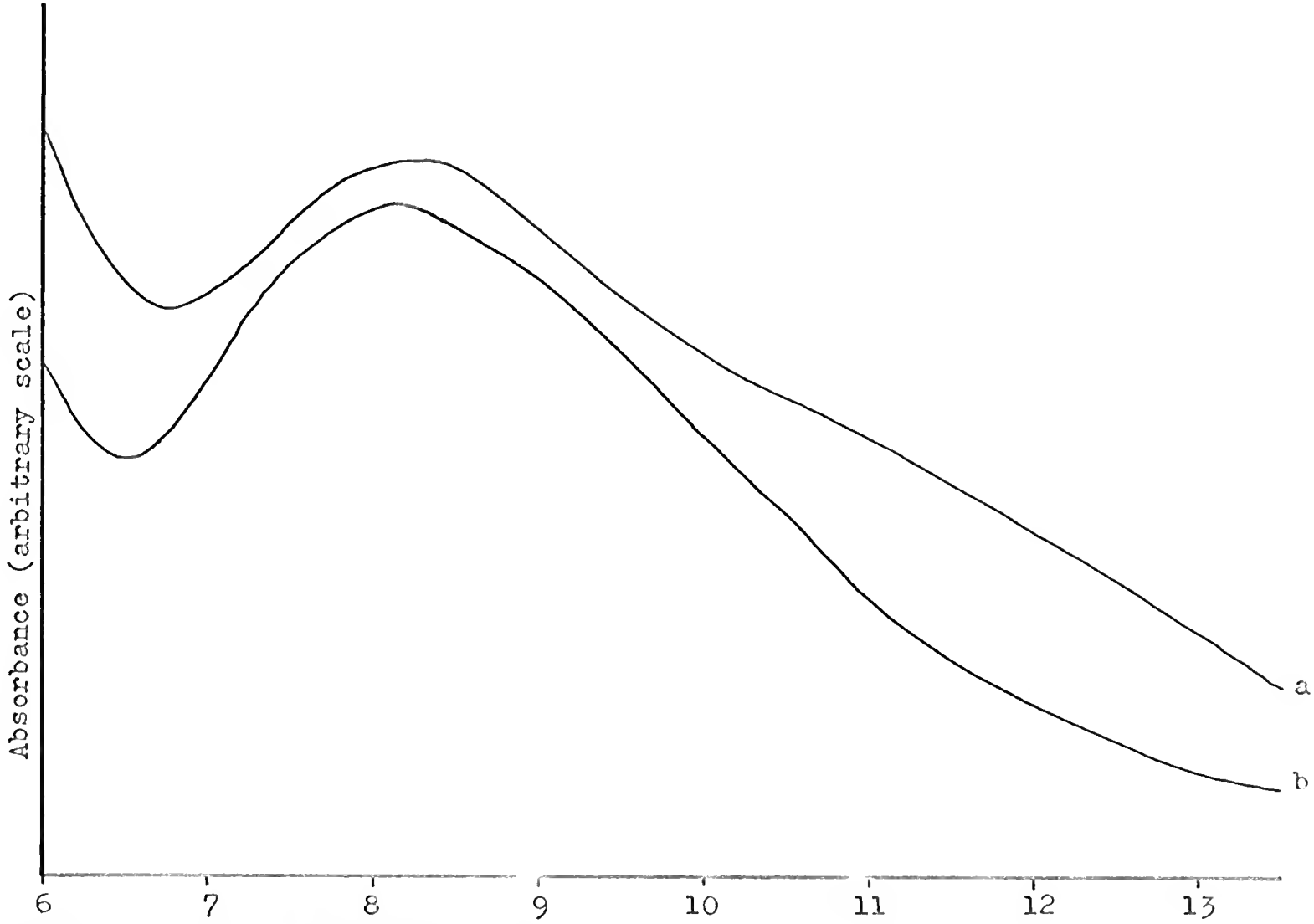

Fig. 4.-Diffuse reflectance spectra of (a) $[NiI_2(PAPI)]$ and (b) $[Ni(H_2O)(PA)(PAPI)](ClO_4)_2$ from 6,000 to 13,500 Å.

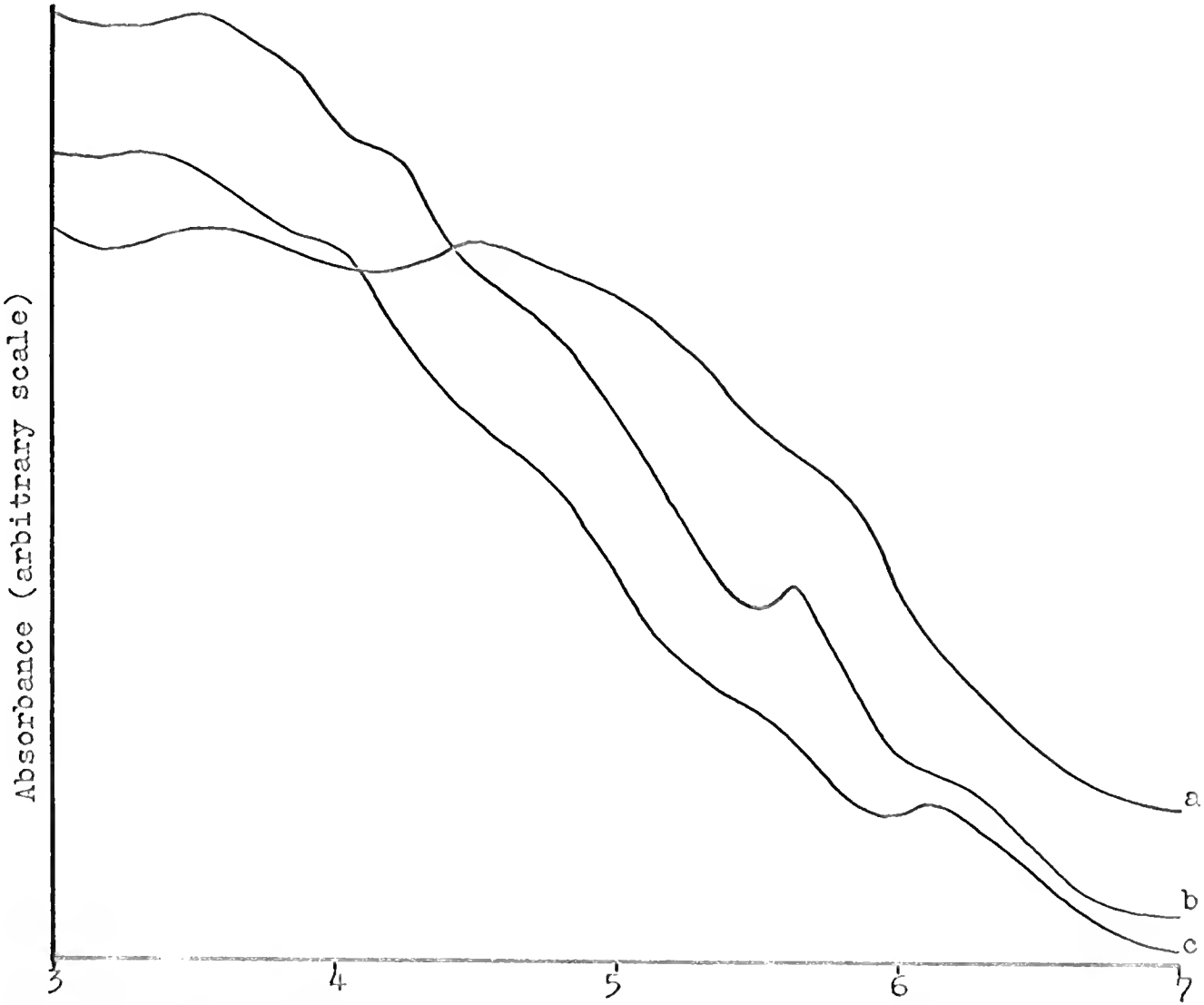

Fig. 5.--Diffuse reflectance spectra of (a) [CoI_2(PAPI)], (b) [$CoBr_2$(PAPI)], and (c) [$CoCl_2$(PAPI)] from 3,000 to 7,000 A.

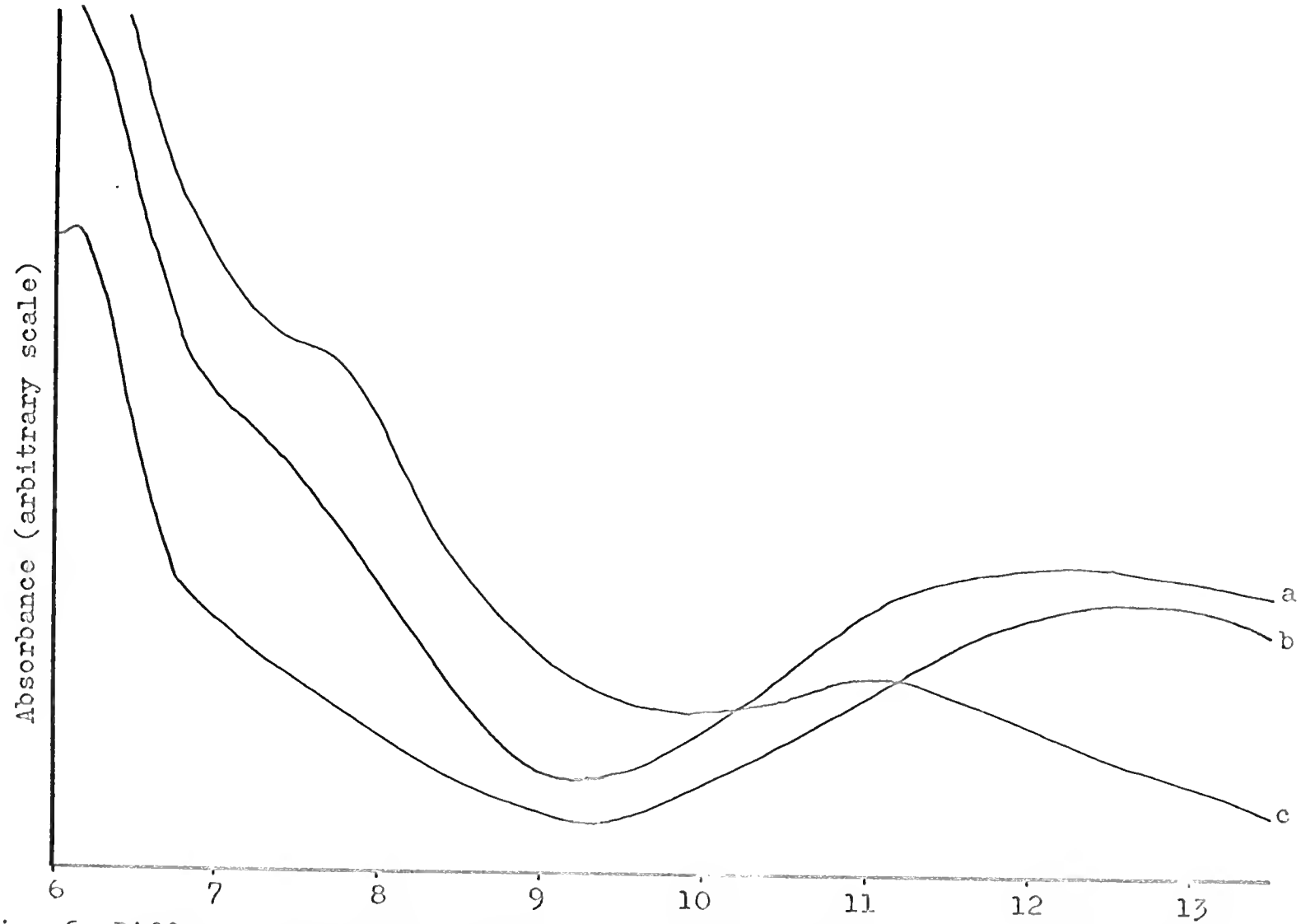

Fig. 6.--Diffuse reflectance spectra of (a) [$CoBr_2$(PAPI)], (b) [$CoCl_2$(PAPI)], and (c) [CoI_2(PAPI)] from 6,000 to 13,500 A.

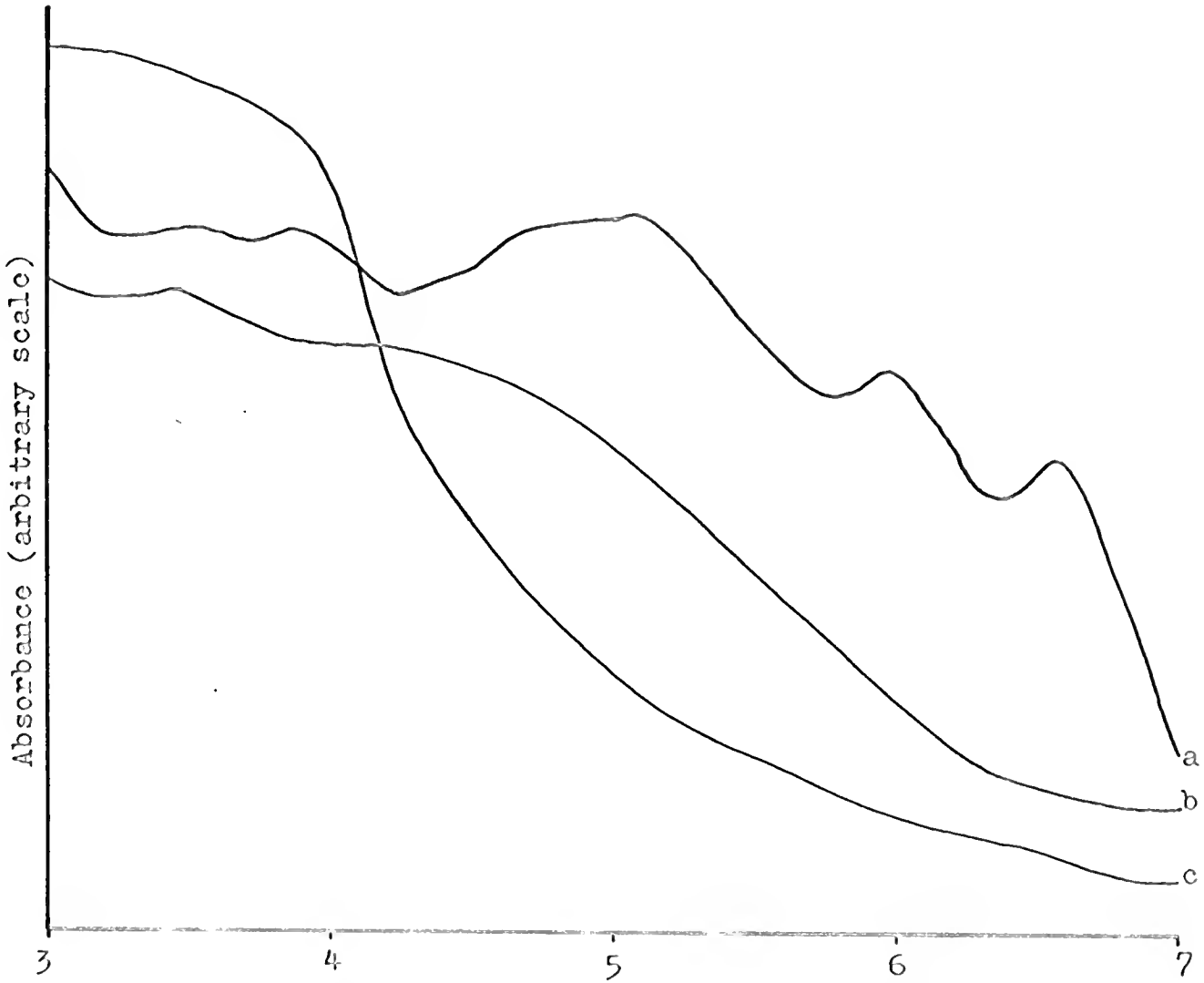

Fig. 7.--Diffuse reflectance spectra of (a) $[Co(ClO_4)_2(PAPI)]$, (b) $[Co(NO_2)_2(PAPI)]$, and (c) $[Co(NCS)_2(PAPI)]$ from 3,000 to 7,000 A.

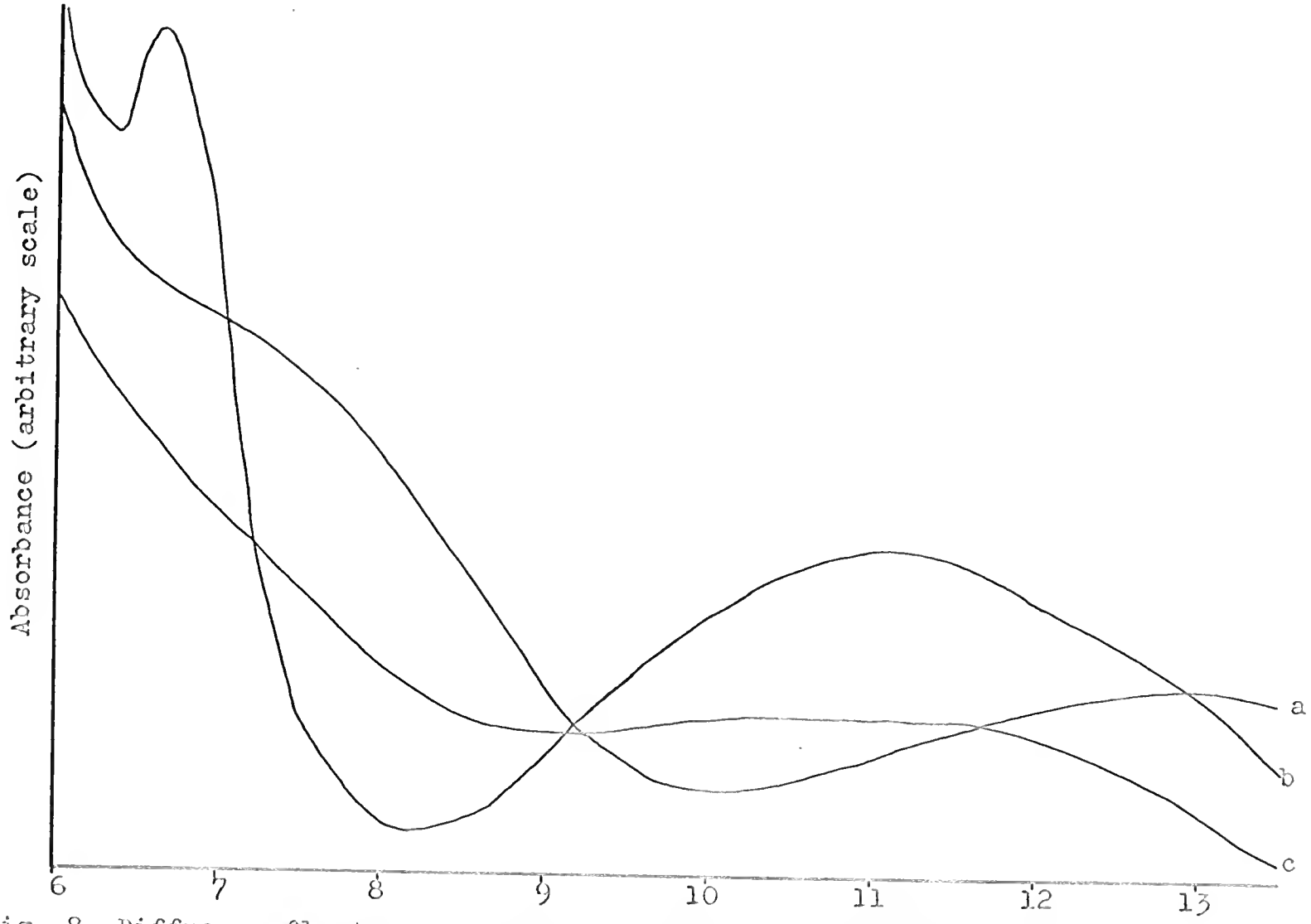

Fig. 8.-Diffuse reflectance spectra of (a) $[Co(NO_2)_2(PAPI)]$, (b) $[Co(ClO_4)_2(PAPI)]$, and (c) $[Co(NCS)_2(PAPI)]$ from 6,000 to 13,500 A.

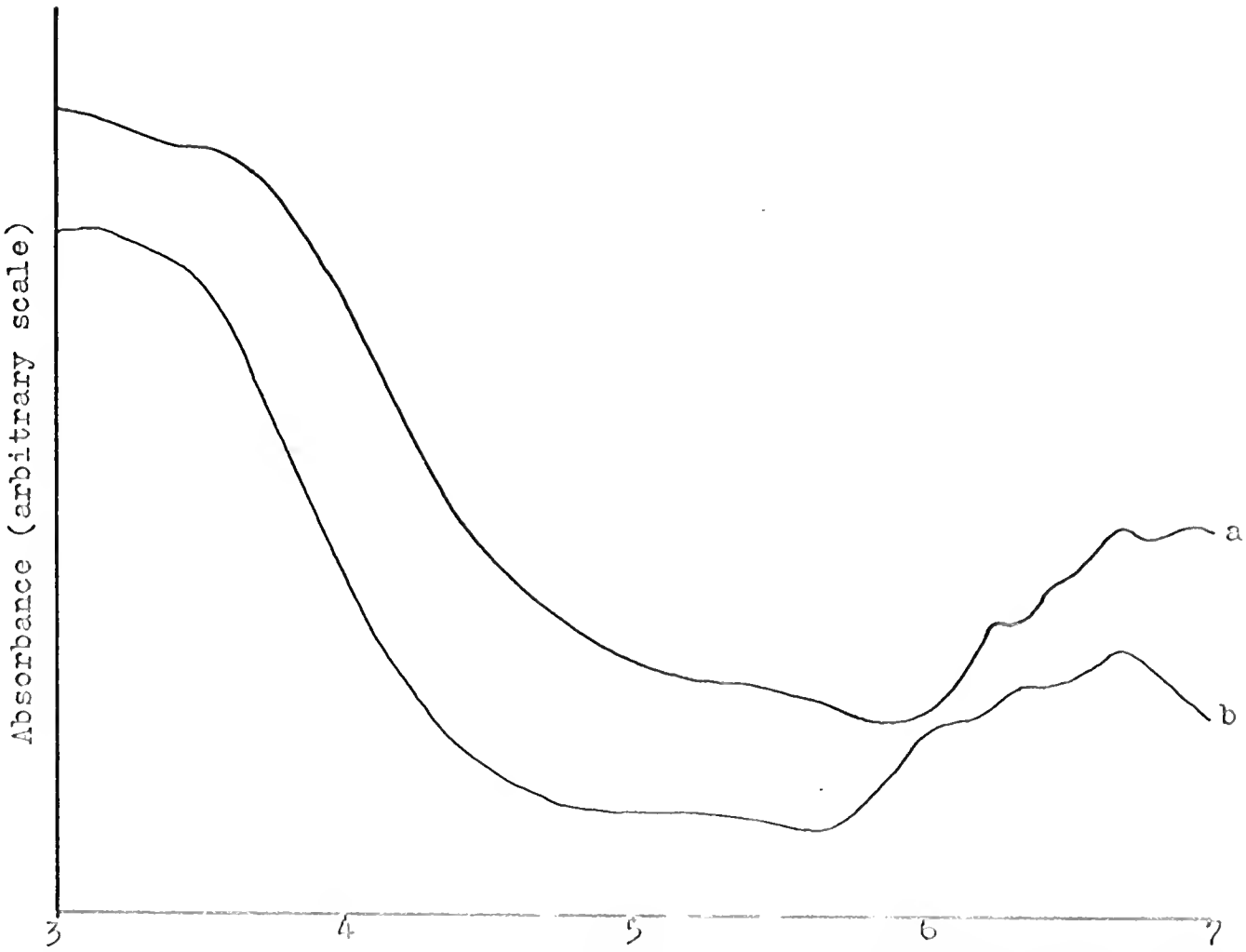

Fig. 9.-Diffuse reflectance spectra of (a) green $CoBr_2$(PAPI) and green $CoCl_2$(PAPI) from 3,000 to 7,000 A.

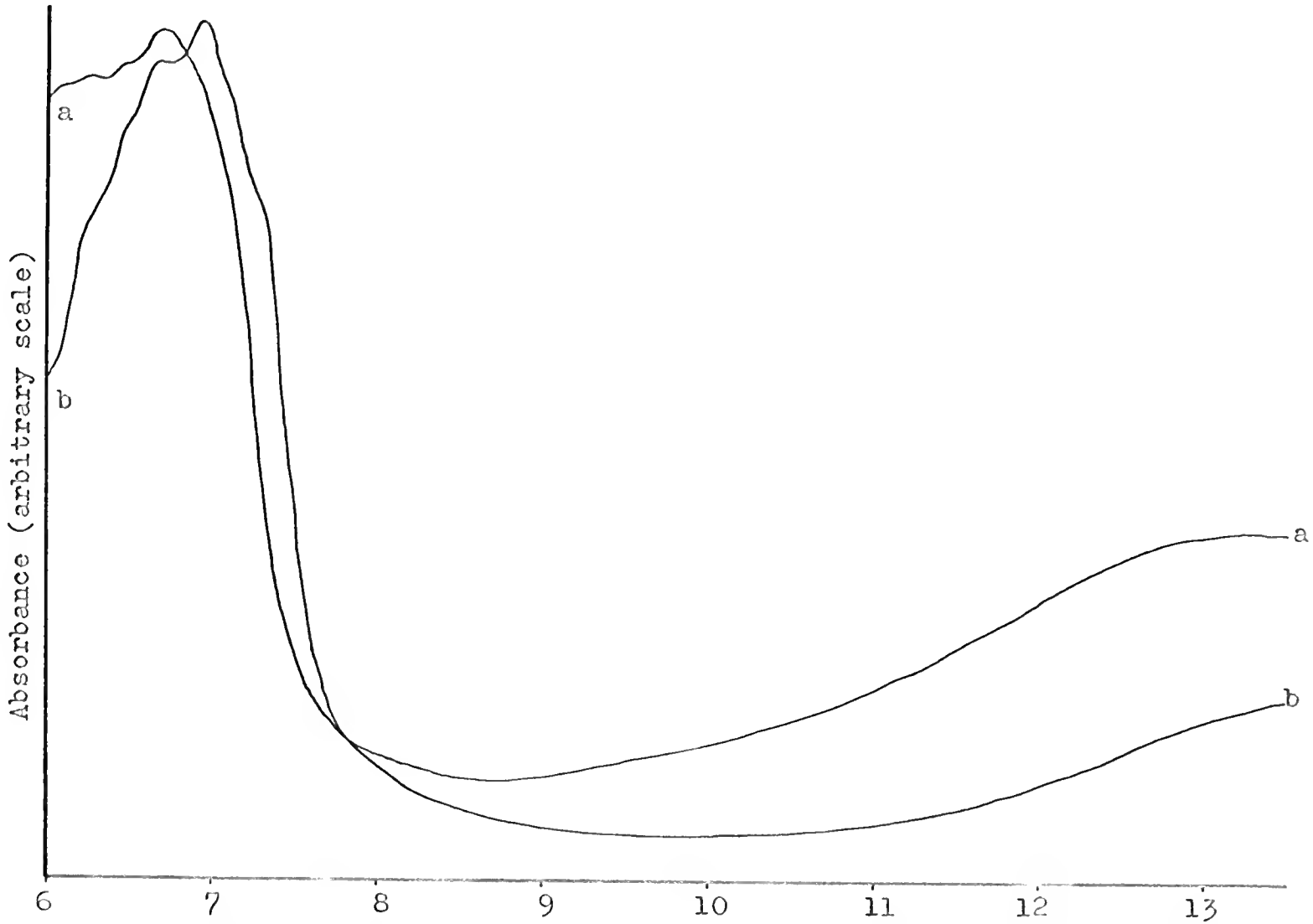

Fig. 10.-Diffuse reflectance spectra of (a) green $CoCl_2$(PAPI) and green $CoBr_2$(PAPI) from 6,000 to 13,500 A.

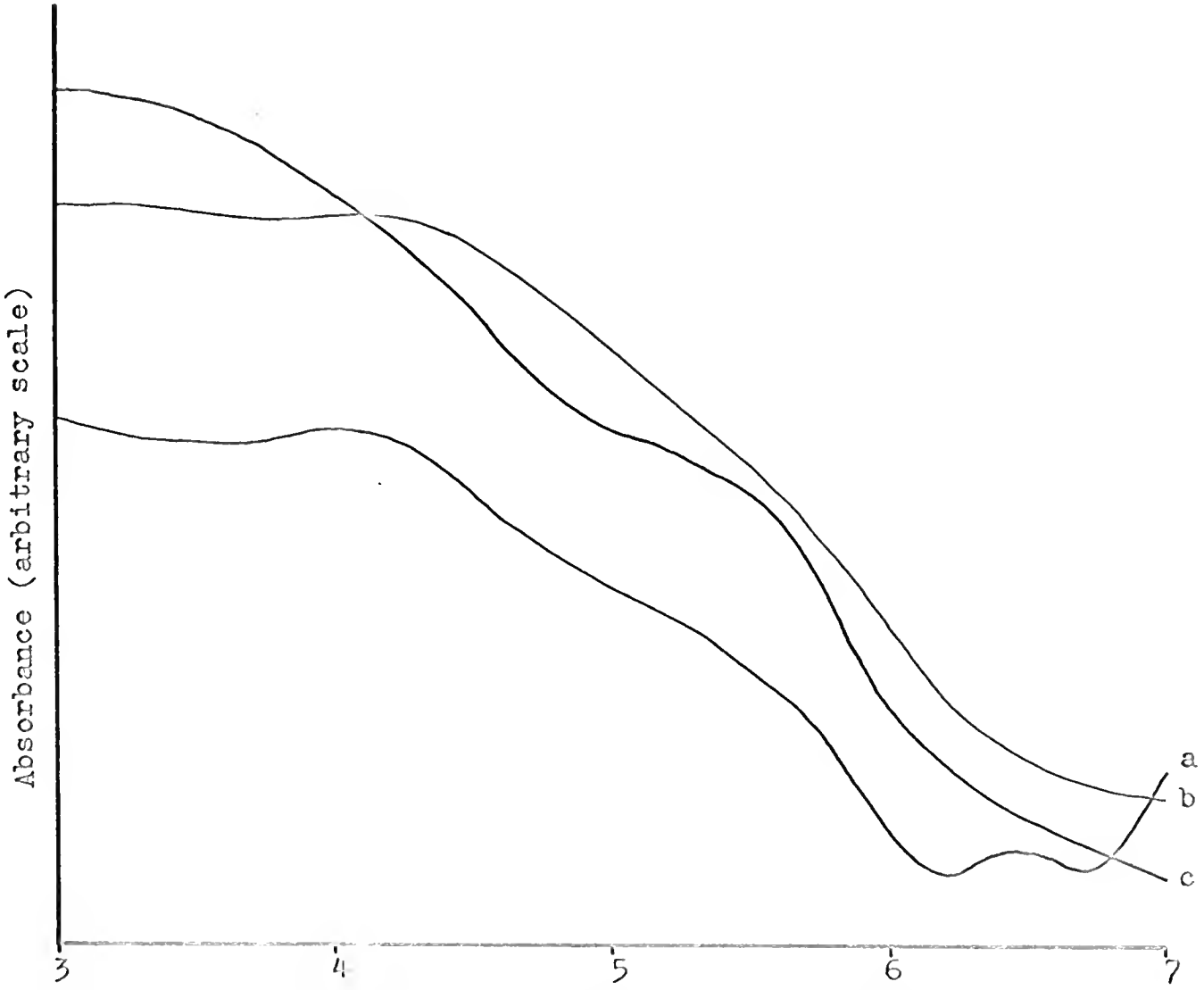

Fig. 11.-Diffuse reflectance spectra of (a) $[CoBr_2(PAT)_2]$, (b) $[CoI_2(PAT)_2]$, and (c) $[CoCl_2(PAT)_2]$ from 3,000 to 7,000 A.

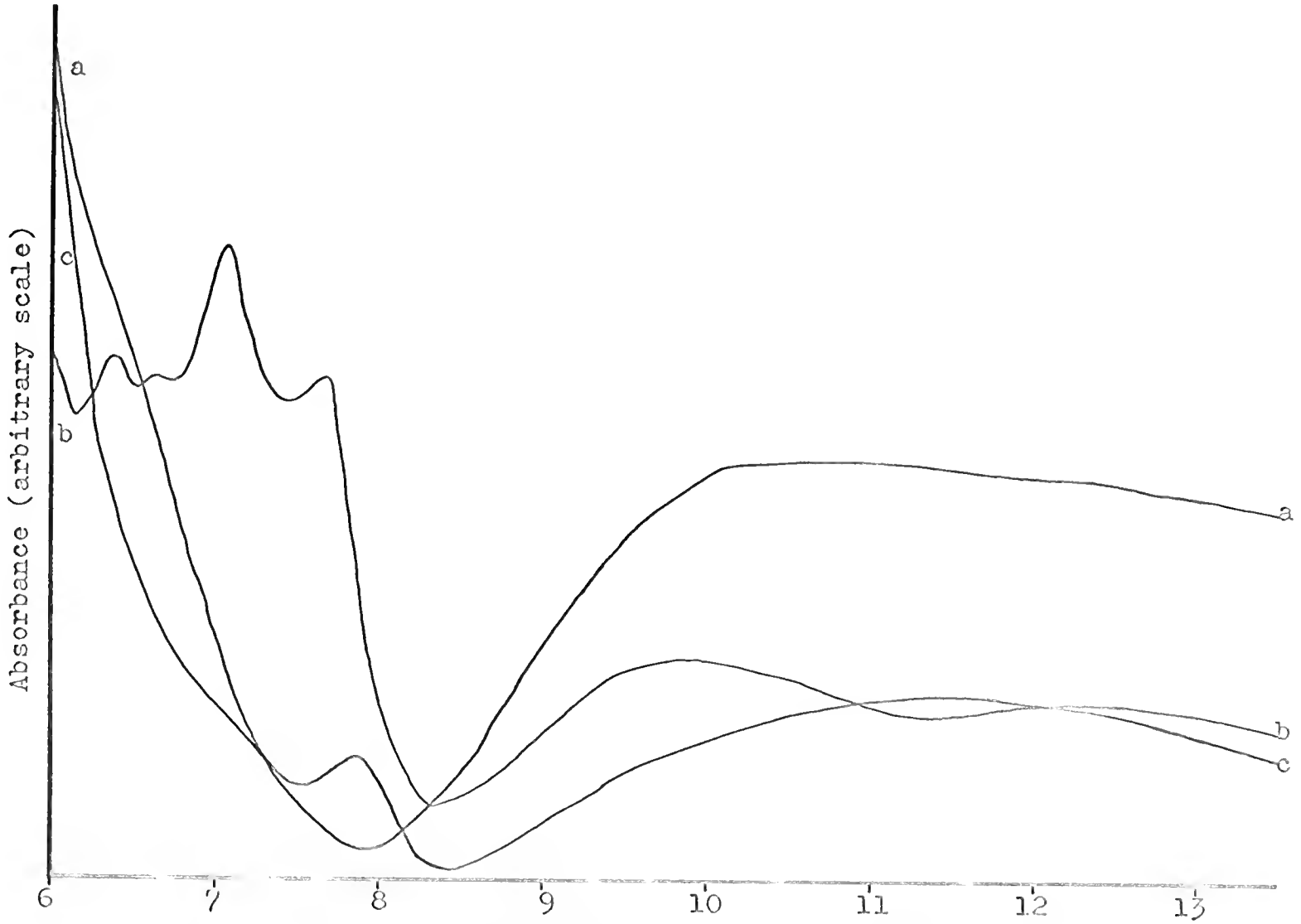

Fig. 12.-Diffuse reflectance spectra of (a) $[CoCl_2(PAT)_2]$, (b) $[CoBr_2(PAT)_2]$, and (c) $[CoI_2(PAT)_2]$ from 6,000 to 13,500 A.

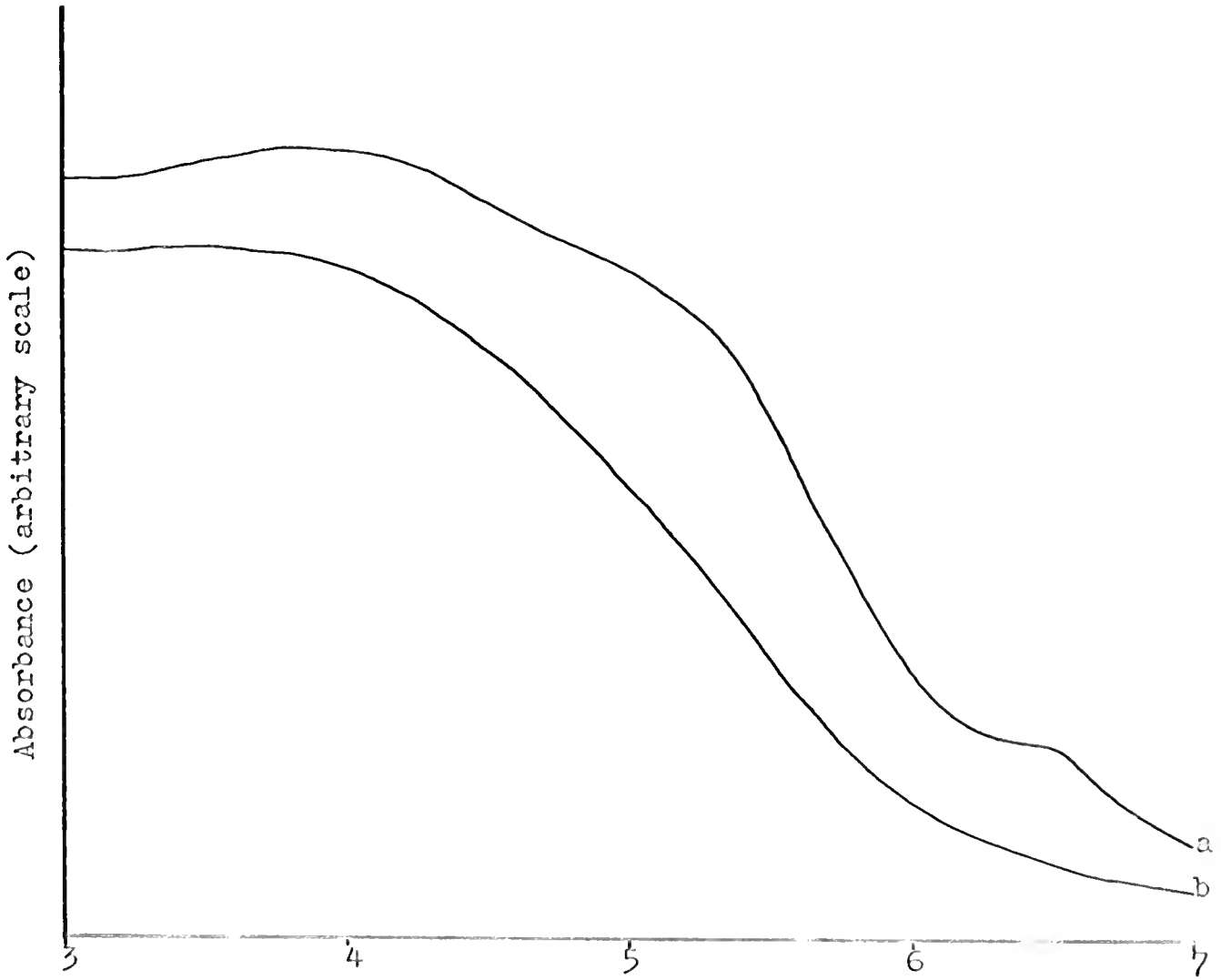

Fig. 13.--Diffuse reflectance spectra of (a) $[Co(NCS)_2(PAT)_2]$ and (b) $[Co(NO_2)_2(PAT)_2]$ from 3,000 to 7,000 A.

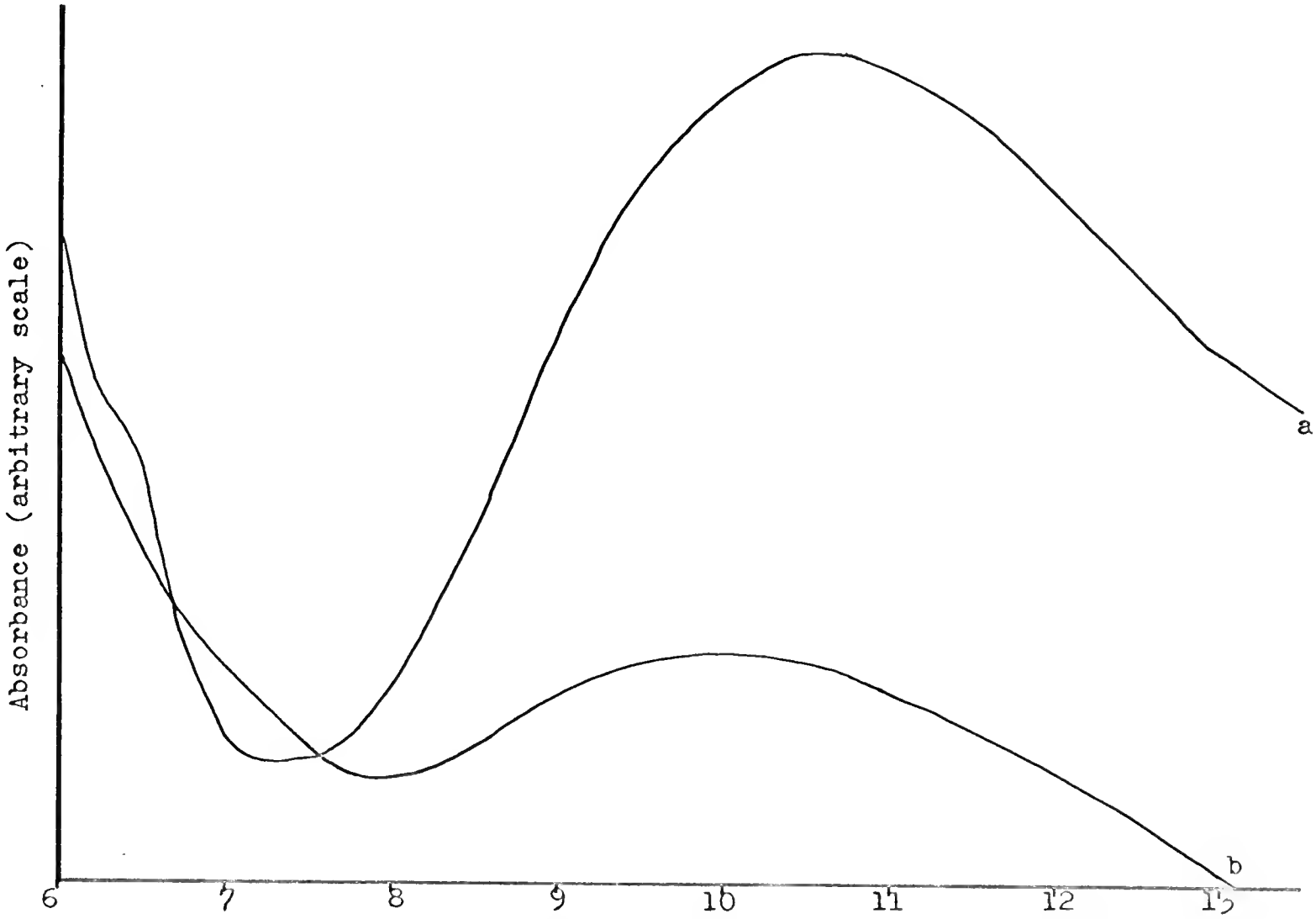

Fig. 14.-Diffuse reflectance spectra of (a) $[Co(NO_2)_2(PAT)_2]$, and (b) $[Co(NCS)_2(PAT)_2]$ from 6,000 to 13,500 A.

TABLE 3

DIFFUSE REFLECTANCE ABSORPTIONS OF NICKEL(II)--PAPI COMPLEXES

Complex	Wavelength, A	Energy, cm^{-1}
$[NiCl_2(PAPI)]\cdot 3/2H_2O$	3,440	29,100
	3,670	27,200
	5,620 (sh)	17,800
	8,120 (sh)	12,300
	9,440	10,600
$[NiBr_2(PAPI)]\cdot 3/2H_2O$	3,450	29,000
	3,810	26,200
	4,870	20,500
	5,500 (sh)	18,200
	8,100 (sh)	12,300
	9,250	10,800
$[NiI_2(PAPI)]$	3,500	28,600
	3,800	26,300
	4,070	24,600
	4,300 (sh)	23,300
	8,250	12,100
	10,500 (sh)	9,500
$[Ni(H_2I)(PA)(PAPI)](ClO_4)_2$	3,120	32,000
	3,370	29,700
	3,570	28,000
	3,900 (sh)	25,600
	4,370 (sh)	22,900
	5,130 (sh)	19,500
	8,130	12,300
	9,370 (sh)	10,700

TABLE 4

DIFFUSE REFLECTANCE ABSORPTIONS OF COBALT(II)--PAPI COMPLEXES

Complex	Wavelength, A	Energy, cm^{-1}
$[CoCl_2(PAPI)]$	3,340	30,000
	3,590 (sh)	27,900
	3,950	25,300
	4,630 (sh)	21,600
	5,500 (sh)	18,200
	6,090	16,400
	7,500 (sh)	13,300
	12,750	7,800
$[CoBr_2(PAPI)]$	3,300	30,300
	3,550	28,200
	3,800	26,300
	4,070 (sh)	24,600
	4,750 (sh)	21.100
	5,620	17,800
	6,250 (sh)	16,000
	7,250 (sh)	13,800
	12,370	8,100
$[CoI_2(PAPI)]$	3,530	28,300
	4,500	22,200
	5,125 (sh)	19,500
	5,770	17,300
	7,750 (sh)	12,900
	11,120	9,000
$[Co(NO_2)_2(PAPI)]$	3,440	29,100
	4,190	23,900
	5,500	18,200
	7,000	14,300
	12,880	7,800
$[Co(NCS)_2(PAPI)]$	3,000	33,300
	5,580 (sh)	17,900
	6,350 (sh)	15,700
	7,130 (sh)	14,000
	10,380	9,600
$[Co(ClO_4)_2(PAPI)]$	3,300	30,300
	3,550	28,200
	3,900	25,600
	5,090	19,600
	5,960	16,800
	6,560	15,200
	11,000	9,100

TABLE 4 - Continued

Complex	Wavelength, A	Energy, cm^{-1}
$CoCl_2$(PAPI) (green)	3,500 (sh)	28,600
	5,200	19,200
	6,120	16,300
	6,370	15,700
	6,520 (sh)	15,300
	6,700	14,900
	7,000 (sh)	14,300
$CoBr_2$(PAPI) (Green)	3,500	28,600
	5,500	18,200
	6,200	16,100
	6,440 (sh)	15,500
	6,680	15,000
	6,940	14,400
	7,300 (sh)	13,700

TABLE 5

DIFFUSE REFLECTANCE ABSORPTIONS OF COBALT(II)--PAT COMPLEXES

Complex	Wavelength, Å	Energy, cm^{-1}
$[CoCl_2(PAT)_2]$	4,120	24,300
	5,380	18,600
	6,250 (sh)	16,000
	10,500	9,500
$[CoBr_2(PAT)_2]$	4,000	25,000
	5,250 (sh)	19,000
	6,400	15,600
	6,670	15,000
	7,100	14,100
	7,770	12,000
	9,900	10,100
$[CoI_2(PAT)_2]$	4,120	24,300
	5,750 (sh)	17,400
	7,880	12,700
	11,500	8,700
$[Co(NO_2)_2(PAT)_2]$	3,500	28,600
	9,750	10,300
$[Co(NCS)_2(PAT)_2]$	3,850	26,000
	5,000 (sh)	20,000
	6,200 (sh)	16,100
	10,600	9,400

The energy level diagram for a d^8 ion in an octahedral field (Figure 15) indicates that three spin-allowed transitions should be observed, namely, from the $^3A_{2g}$ ground state to the excited states $^3T_{2g}$, $^3T_{1g}$, and $^3T_{1g}(^3P)$. The energy separating the ground state from the first two excited states is Δ and 1.8 Δ, respectively. The energy from the ground state to the third excited state is dependent upon the multiplet separation between the ^3F and ^3P terms which varies considerably as the degree of covalent bonding between the ligand and the metal ion varies. Robinson *et al.* have observed that this third transition is obscured by intense charge transfer bands in complexes formed ligands containing the dimethine linkage (39). In addition to the three spin-allowed transitions noted above, the spin-forbidden transition ($^3A_{2g} \rightarrow {}^1E_g$) is frequently observed (17,39).

Assignments of the transitions recorded in Table 6 were made on the basis of internally consistent ligand field energy separations and previous observations.

The Δ values exhibited by the nickel(II) complexes discussed herein (Table 6) are considerably smaller than those exhibited by nickel(II) complexes which are coordinated with *six* unsaturated nitrogen atoms (17,39). This observation is in accordance with the principle of an average environment (24) which is given by the formula,

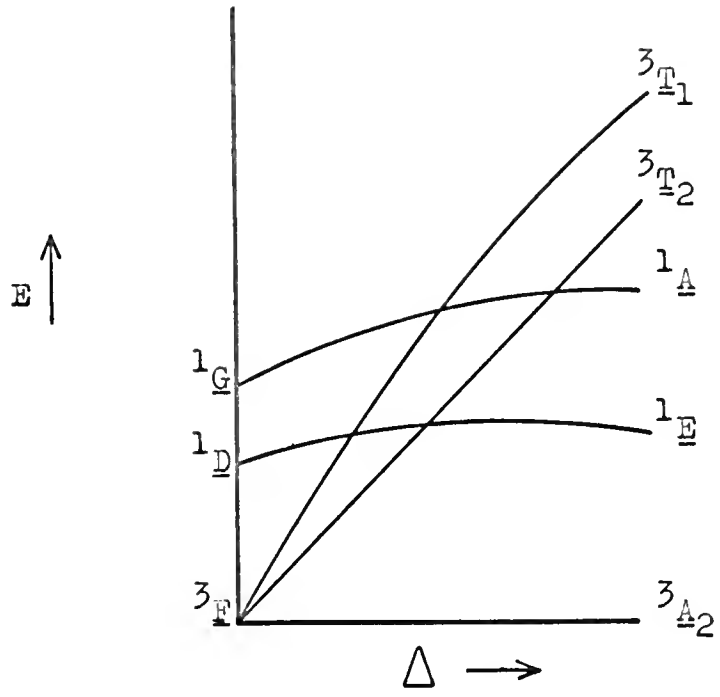

Fig. 15.-Partial energy level diagram for the d^8 configuration in an octahedral field.

TABLE 6

ASSIGNMENTS OF SPECTRAL TRANSITIONS OF NICKEL(II)--PAPI COMPLEXES

Complex	Energy, cm^{-1}	Transition	Δ, cm^{-1}
$[NiCl_2(PAPI)] \cdot 3/2H_2O$	10,600	$^3A_{2g} \longrightarrow {}^3T_{2g}$	10,600
	12,300	$^3A_{2g} \longrightarrow {}^1E_g$	
	17,800	$^3A_{2g} \longrightarrow {}^3T_{1g}$	
$[NiBr_2(PAPI)] \cdot 3/2H_2O$	10,800	$^3A_{2g} \longrightarrow {}^3T_{2g}$	10,800
	12,300	$^3A_{2g} \longrightarrow {}^1E_g$	
	18,200	$^3A_{2g} \longrightarrow {}^3T_{1g}$	
	20,500		
$[NiI_2(PAPI)]$	9,500	$^3A_{2g} \longrightarrow {}^1E_g$	
	12,100	$^3A_{2g} \longrightarrow {}^3T_{2g}$	12,100
$[NI(H_2O)(PA(PAPI)](ClO_4)2$	10,700	$^3A_{2g} \longrightarrow {}^1E_g$	
	12,300	$^3A_{2g} \longrightarrow {}^3T_{2g}$	12,300
	19,500	$^3A_{2g} \longrightarrow {}^3T_{1g}$	
	22,900		

$$\Delta MA_nB_{6-n} = n\Delta MA_6/6 + 6-n\Delta MB_6/6 ,$$

where ΔMA_6 and ΔMB_6 represent the field strengths characteristic of purely hexacoordinated species. Thus, the smaller basicities of the anions in these complexes relative to those of unsaturated nitrogen atoms serve to decrease the average value of Δ.

Aside from the over-all decrease in the field strengths, the ligand fields produced by the halide ions with nickel(II) and cobalt(II) are expected to increase in the order I < Br < Cl (class a metal behavior) because of the positions of the halide ions in the spectrochemical series. Contrary to expectations, the ligand fields exhibited by the nickel-halide complexes reported here increase in the reverse order (Table 6). This observation, however, is not totally without precedence. Melson and Busch found also that within a series of tetragonally distorted complexes the iodo complex exhibits a larger Δ value than does the chloro or bromo complex (32). The chloro complex, however, exhibited a Δ value slightly larger than that exhibited by the bromo complex. They attributed the small fields produced by the chloro and bromo complexes to a reduction of the ligand fields caused by an interaction of the chloride ion and the bromide ion with the molecule of water present in each of the complexes, that is, water is hydrogen bonded between ions. Both the chloro and bromo

complexes contained a molecule of water which could not be removed without decomposition of the complex.

The chloro and bromo complexes prepared during the course of this investigation also contain water which can not be removed *in vacuo* at 200°C over P_4O_{10}. Because of this similarity in constitution between these complexes and those reported by Melson and Busch, the observed ligand field trends can be rationalized also in terms of hydrogen-bonded water; however, doubt is cast on this explanation by the fact that the octahedral cobalt(II)-PAPI-halo complexes which do not contain water exhibit a similar ligand field trend (Table 7).

An alternate explanation of the observed behavior may be based upon a reversal in the metal character, that is, becoming a class b metal. Upon coordination, the ligand may donate sufficient electron density to the metal which can in turn back-donate some of this electron density to the ligand d-orbitals. For class b metals, the strength of the metal-halide bond varies in the order I > Br > Cl. This order is due to the relative energies of the d-orbitals which accept the back-donation and thereby form a second bond. The d-orbitals which are closer in energy to that of the metal orbital, form the stronger bond.

Examples exist for such a reversal in metal character. Ferrous chloride, for example, will not coordinate with

carbon monoxide; however, coordinated ferrous ion (hemoglobin) forms very strong bonds to carbon monoxide. This strong bond has been explained on the basis of additional bonding between the metal and the carbon monoxide resulting from a back-donation of electron density from the metal to the antibonding orbitals on the ligand. The same situation may exist with the nickel(II) (and cobalt(II), vide infra) complexes. However, further investigation is required before a more definite assertion can be made.

The triplet-singlet transition in the spectra of the nickel(II) complexes was observed as ill-defined shoulders on the low energy absorption band. This position of the transition conforms to observations reported by Robinson et al., that is, it appears on the high energy side of the band for Δ values below 12,100 cm^{-1} and on the low energy side for higher values (39).

The absorption attributed to the $^3A_{2g} \rightarrow {}^3T_{1g}$ transition appears as a very slight shoulder on the intense charge transfer band which trails down across the visible region from the ultraviolet. This absorption in the spectra of the bromo and the perchlorate complex appears to be split. It could not be ascertained whether or not this splitting was due to a larger distortion within these complexes. In fact, the chloro complex which exhibits essentially the same Δ value as that by the bromo complex does not manifest any splitting of this absorption.

The visible spectra of cobalt(II) complexes have not been interpreted as completely as have those of the analogous nickel(II) complexes. The absorption maxima are less well defined and furthermore, the maxima do not conform as closely to the ligand field predictions. The energy diagram (Figure 16) for a high spin $\underline{d}^7$ ion shows that three transitions should be observed, namely, from the ground state $^4\underline{T}_{1g}$ to the excited states $^4\underline{T}_{2g}$, $^4\underline{A}_{2g}$, and $^4\underline{T}_{1g}(^4\underline{P})$, the energies corresponding to 0.8 Δ, 1.8 Δ, and 15,400 cm^{-1} + 0.6 Δ, respectively. The value, 15,400 cm^{-1} is the multiplet separation between the $^4\underline{F}$ and $^4\underline{P}$ states of the free ion; this value will be somewhat smaller in the complexed ion due to covalent bonding effects.

The assignments which were made for some of the transitions are listed in Table 7. The octahedral PAPI complexes containing halide ions exhibit the same ligand field trend as that exhibited by the nickel-halo complexes. The Δ values exhibited by the nickel(II) complexes, however, are somewhat larger than those of the corresponding cobalt(II) complexes. This observation is contrary to that which has been observed previously. The pronounced absorptions in the spectrum of the perchlorato complex are suspected of being due to transitions between doublet states; however, no definite assignments can be made. Definite assignments of many of the remaining absorptions in the spectra of the complexes can not be made.

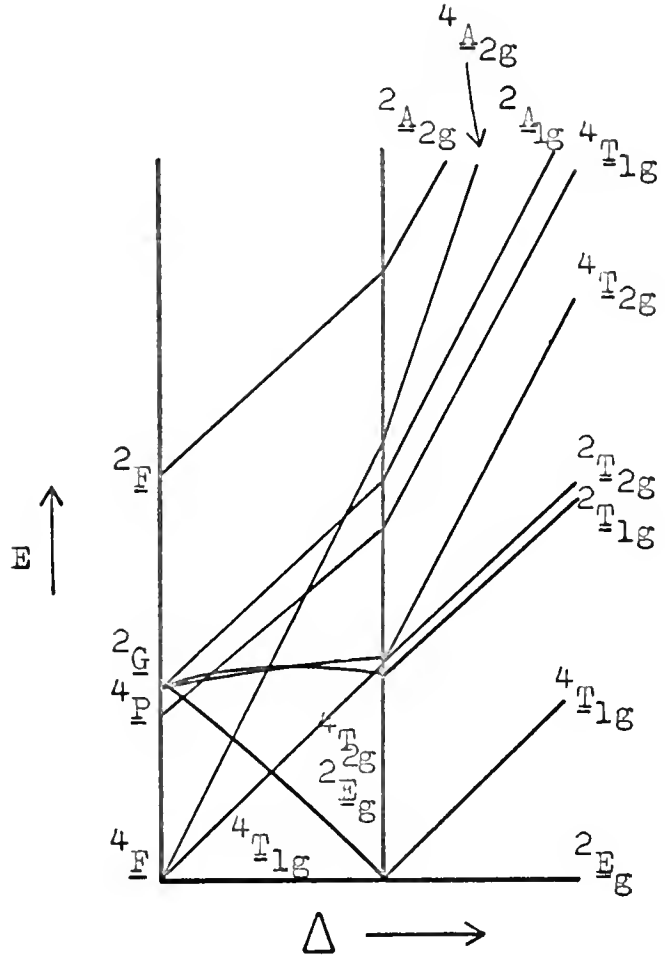

Fig. 16.-Energy level diagram for the d^7 configuration in an octahedral field.

TABLE 7

ASSIGNMENTS OF SPECTRAL TRANSITIONS OF COBALT(II)--PAPI COMPLEXES

Complex	Energy, cm^{-1}	Transition	Δ, cm^{-1}
$[CoCl_2(PAPI)]$	7,800	$^4\underline{T}_{1g} \longrightarrow {}^4\underline{T}_{2g}$	9,800
$[CoBr_2(PAPI)]$	8,100	$^4\underline{T}_{1g} \longrightarrow {}^4\underline{T}_{2g}$	10,100
$[CoI_2(PAPI)]$	9,000	$^4\underline{T}_{1g} \longrightarrow {}^4\underline{T}_{2g}$	11,200
$[Co(NO_2)_2(PAPI)]$	7,800	$^4\underline{T}_{1g} \longrightarrow {}^4\underline{T}_{2g}$	9,800
$[Co(NCS)_2(PAPI)]$	9,600	$^4\underline{T}_{1g} \longrightarrow {}^4\underline{T}_{2g}$	12,000
$[Co(ClO_4)_2(PAPI)]$	9,100	-----	---
$ClCl_2(PAPI)$ (green)	14,900	$^4\underline{A}_{2g} \longrightarrow {}^4\underline{T}_{1g}(^4\underline{P})$	---
$CoBr_2(PAPI)$ (Green)	14,400	$^4\underline{A}_{2g} \longrightarrow {}^4\underline{T}_{1g}(^4\underline{P})$	---

The spectra of the two green PAPI complexes are characteristic of tetrahedral complexes, that is, the intense multicomponent absorption near 6,500 A (Figure 10) is characteristic of tetrahedrally coordinated cobalt(II) and is assigned, therefore, to the transition $^4\underline{A}_{2g} \longrightarrow {}^4\underline{T}_{1g}(^4\underline{P})$ (3,22,23). This absorption lies at longer wavelengths in the bromo complex than in the chloro complex, consistent with the behavior noted previously (9,10,11,12, 19,41). The pure iodo complex of this tetrahedral PAPI series was never obtained; but, a reflectance spectrum of the impure material exhibits the characteristic absorption at still longer wavelengths. These data provide strong evidence that at least one of the two halide ions is coordinated to the metal. If a halide ion were not coordinated, the position of this absorption should be unchanged within the series of complexes.

Interpretation of the visible spectra of the PAT complexes is made difficult by the fact that cis-trans isomers can exist within the series of complexes. The spectra of a cis-complex should exhibit a characteristic broadening of the absorption maxima, whereas, the spectra of a trans-complex should exhibit a splitting of some absorption maxima. With a mixture of these isomers, therefore, the resultant spectrum would probably be poorly defined with broad maxima. This behavior was observed in

the spectra of the PAT complexes. An intense charge transfer absorption which trails across the visible region from the ultraviolet also obscures some of the absorption maxima. Nonetheless, some spectral assignments are listed in Table 8.

The bromo complex has an intense absorption at approximately 7,000 A which is suggestive of a tetrahedral complex. After heating this complex, its spectrum no longer exhibits this absorption but rather is similar to the spectra of the other complexes in the series. During the determination of the temperature dependence of the magnetic susceptibility of this complex (Figure 22), it was observed that the sample began to lose weight at approximately 66°C. This loss in weight is probably due to a small amount of solvent displaced from the sample. A differential thermal analysis on this complex also indicated an absorption of energy at this temperature. The amount of solvent present in the complex, however, must be negligible since the analytical results did not indicate any solvent to be present. This small amount of solvent may induce some of the molecules to assume a tetrahedral environment and thereby giving rise to the observed absorption.

TABLE 8

ASSIGNMENTS OF SPECTRAL TRANSITIONS OF COBALT(II)--PAT COMPLEXES

Complex	Energy, cm^{-1}	Transition	Δ, cm^{-1}
$[CoCl_2(PAT)_2]$	9,500	$^4T_{1g} \longrightarrow {}^4T_{2g}$	11,900
$[CoBr_2(PAT)_2]$	10,100	$^4T_{1g} \longrightarrow {}^4T_{2g}$	12,600
$[CoI_2(PAT)_2]$	8,700	$^4T_{1g} \longrightarrow {}^4T_{2g}$	10,900
$[Co(NO_2)_2(PAT)_2]$	10,300	$^4T_{1g} \longrightarrow {}^4T_{2g}$	12,900
$[Co(NCS)_2(PAT)_2]$	9,400	$^4T_{1g} \longrightarrow {}^4T_{2g}$	11,800

Magnetic measurements

Temperature dependent magnetic susceptibilities were measured at two different field strengths for each of the cobalt(II) complexes prepared during the course of this investigation. The magnetic susceptibilities were corrected for the diamagnetism of the ligands. These diamagnetic corrections are listed in Appendix II. The corrected temperature dependent molar susceptibilities are listed in Tables 9 through 20. A plot of $1/\chi_c$ vs T for each complex is presented in Figures 17 through 24. The magnetic moment of each of the cobalt(II) complexes together with the appropriate Curie and Weiss constants is listed in Table 21. The slopes of the $1/\chi_c$ vs T plots were determined graphically; the Curie constants were obtained by taking the reciprocal of this slope. The Weiss constants were determined analytically. Room temperature moments for each of the nickel(II) complexes were determined at two different field strengths and are listed in Table 22.

The six-coordinate cobalt(II) complexes (the perchlorato complex excepted) exhibit normal magnetic moments (see Introduction). The agreement of the magnetic moments at the two different field strengths indicates that the metal ions are magnetically dilute, that is, no metal-metal interactions exist.

TABLE 9

TEMPERATURE DEPENDENCE OF THE MOLAR SUSCEPTIBILITY AND MAGNETIC MOMENT OF $[CoCl_2(PAPI)]$

T, °K	$\chi_c \times 10^6$ (cgs units)	μ_{eff} (Bohr magnetons)
113.01	24,894	4.76
122.63	23,203	4.79
140.64	20,595	4.83
160.66	18,124	4.85
178.67	16,363	4.85
189.37	15,467	4.86
212.33	13,822	4.86
295.80	9,822	4.84
314.17	9,219	4.83
329.83	8,783	4.83
348.90	8,269	4.82
363.97	7,915	4.82
379.76	7,570	4.81
397.99	7,198	4.81

TABLE 10

TEMPERATURE DEPENDENCE OF THE MOLAR SUSCEPTIBILITY AND MAGNETIC MOMENT OF [$CoBr_2$(PAPI)]

T, °K	$\chi_c \times 10^6$(cgs units)	μ_{eff}(Bohr magnetons)
111.50	25,051	4.75
128.37	22,185	4.79
146.31	19,672	4.82
164.25	17,695	4.84
182.19	16,038	4.85
200.06	14,563	4.85
217.93	13,462	4.86
295.72	9,816	4.84
314.81	9,167	4.83
332.75	8,679	4.83
357.73	8,069	4.83
375.45	7,668	4.82
393.68	7,321	4.82
399.93	7,160	4.81

TABLE 11

TEMPERATURE DEPENDENCE OF THE MOLAR SUSCEPTIBILITY AND MAGNETIC MOMENT OF $[CoI_2(PAPI)]$

T, °K	$\chi_c \times 10^6$(cgs units)	μ_{eff}(Bohr magnetons)
113.87	23,843	4.68
128.22	21,644	4.73
142.58	19,679	4.76
156.93	17,923	4.76
171.28	16,457	4.77
192.81	14,634	4.81
214.34	13,263	4.79
290.20	9,662	4.75
307.28	9,124	4.75
318.04	8,729	4.73
335.98	8,225	4.72
353.93	7,842	4.73
371.87	7,435	4.72
389.81	7,075	4.72
401.72	6,852	4.71

TABLE 12

TEMPERATURE DEPENDENCE OF THE MOLAR SUSCEPTIBILITY AND MAGNETIC MOMENT OF $[Co(NO_2)_2(PAPI)]$

T, °K	$\chi_c \times 10^6$ (cgs units)	μ_{eff} (Bohr magnetons)
113.37	19,621	4.23
124.99	18,056	4.27
139.35	16,320	4.28
156.57	14,672	4.31
174.51	13,336	4.33
192.45	12,171	4.35
210.40	11,187	4.36
294.65	8,106	4.39
310.15	7,729	4.40
328.59	7,326	4.40
346.17	6,992	4.42
365.55	6,627	4.42
382.99	6,307	4.41
398.92	6,045	4.41

TABLE 13

TEMPERATURE DEPENDENCE OF THE MOLAR SUSCEPTIBILITY AND MAGNETIC MOMENT OF $[Co(NCS)_2(PAPI)]$

T, °K	$\chi_c \times 10^6$ (cgs units)	μ_{eff} (Bohr magnetons)
112.58	22,608	4.53
124.28	20,620	4.55
138.63	18,757	4.58
152.98	17,166	4.60
167.34	15,750	4.61
181.69	14,544	4.62
196.04	13,497	4.62
210.40	12,631	4.63
296.87	8,931	4.62
310.87	8,502	4.62
327.01	8,101	4.62
343.16	7,733	4.63
361.10	7,311	4.62
379.04	6,953	4.61
396.98	6,596	4.60

TABLE 14

TEMPERATURE DEPENDENCE OF THE MOLAR SUSCEPTIBILITY AND MAGNETIC MOMENT OF $[Co(ClO_4)_2(PAPI)]$

T, °K	$\chi_c \times 10^6$ (cgs units)	μ_{eff} (Bohr magnetons)
114.23	4,209	1.97
124.28	3,949	1.99
138.63	3,588	2.00
152.98	3,298	2.02
167.34	3,085	2.04
181.69	2,875	2.05
196.04	2,746	2.08
210.40	2,598	2.10
224.75	2,530	2.14
242.69	2,450	2.19
256.47	2,419	2.24
284.10	2,425	2.36
296.51	2,490	2.44
310.87	2,585	2.55
325.22	2,721	2.67
339.57	2,854	2.80
353.93	3,073	2.96
368.28	3,326	3.14
382.63	3,635	3.35
399.14	4,014	3.60

TABLE 15

TEMPERATURE DEPENDENCE OF THE MOLAR SUSCEPTIBILITY AND MAGNETIC MOMENT OF $CoBr_2$(PAPI)(GREEN)

T, °K	$\chi_c \times 10^6$(cgs units)	μ_{eff}(Bohr magnetons)
107.48	20,272	4.19
124.28	17,911	4.24
138.63	16,324	4.27
152.98	14,950	4.29
167.34	13,845	4.32
181.69	12,832	4.34
196.04	11,960	4.35
210.40	11,228	4.37
293.28	8,191	4.40
303.69	7,916	4.40
318.04	7,611	4.42
332.40	7,284	4.42
346.75	7,020	4.43
361.10	6,756	4.44
375.45	6,577	4.46
389.81	6,348	4.47
404.16	6,196	4.49

TABLE 16

TEMPERATURE DEPENDENCE OF THE MOLAR SUSCEPTIBILITY AND MAGNETIC MOMENT OF $[CoCl_2(PAT)_2]$

T, °K	$\chi_c \times 10^6$(cgs units)	μ_{eff}(Bohr magnetons)
110.57	22,497	4.48
140.71	18,367	4.57
170.85	15,298	4.59
182.21	14,179	4.56
199.56	13,048	4.58
296.71	8,992	4.64
325.94	8,204	4.64
356.08	7,587	4.67
386.22	6,978	4.66
395.69	6,810	4.66

TABLE 17

TEMPERATURE DEPENDENCE OF THE MOLAR SUSCEPTIBILITY AND MAGNETIC MOMENT OF $[CoBr_2(PAT)_2]$

T, °K	$\chi_c \times 10^6$ (cgs units)	μ_{eff} (Bohr magnetons)
110.57	21,021	4.33
124.28	19,038	4.37
138.63	17,228	4.39
152.98	15,765	4.41
167.34	14,529	4.43
181.69	13,376	4.43
196.04	12,388	4.42
210.40	11,613	4.44
289.19	8,508	4.46
297.02	8,233	4.44
310.87	7,887	4.45
325.22	7,520	4.44
339.57	7,312	4.48
353.93	7,085	4.50
382.63	6,598	4.51
396.98	6,346	4.51

TABLE 18

TEMPERATURE DEPENDENCE OF THE MOLAR SUSCEPTIBILITY AND MAGNETIC MOMENT OF $[CoI_2(PAT)_2]$

T, °K	$\chi_c \times 10^6$(cgs units)	μ_{eff}(Bohr magnetons)
108.49	23,032	4.49
124.28	20,521	4.54
138.63	18,739	4.58
152.98	17,238	4.61
167.34	15,909	4.63
196.04	13,787	4.67
210.40	12,939	4.69
292.06	9,393	4.70
303.69	9,065	4.71
318.04	8,657	4.71
332.40	8,279	4.71
346.75	7,940	4.71
361.10	7,630	4.71
375.45	7,350	4.72
389.81	7,042	4.71
404.16	6,718	4.68

TABLE 19

TEMPERATURE DEPENDENCE OF THE MOLAR SUSCEPTIBILITY AND MAGNETIC MOMENT OF $[Co(NO_2)_2(PAT)_2]$

T, °K	$\chi_c \times 10^6$ (cgs units)	μ_{eff} (Bohr magnetons)
108.27	21,132	4.30
122.63	18,926	4.33
136.98	17,155	4.35
151.33	15,563	4.36
165.69	14,335	4.38
195.63	12,267	4.40
210.18	11,498	4.42
224.50	10,810	4.42
296.36	8,246	4.44
326.65	7,522	4.45
356.80	6,893	4.45
386.94	6,285	4.43
400.57	6,086	4.43

TABLE 20

TEMPERATURE DEPENDENCE OF THE MOLAR SUSCEPTIBILITY AND MAGNETIC MOMENT OF $[Co(NCS)_2(PAT)_2]$

T, °K	$\chi_c \times 10^6$ (cgs units)	μ_{eff} (Bohr magnetons)
111.36	21,726	4.42
124.28	19,668	4.44
138.63	17,914	4.48
152.98	16,428	4.50
167.34	15,057	4.51
181.69	13,962	4.52
196.04	13,006	4.54
210.40	12,099	4.53
296.51	8,676	4.56
310.87	8,306	4.57
325.22	7,954	4.57
339.55	7,636	4.57
353.93	7,322	4.57
382.63	6,783	4.58
396.98	6,550	4.58

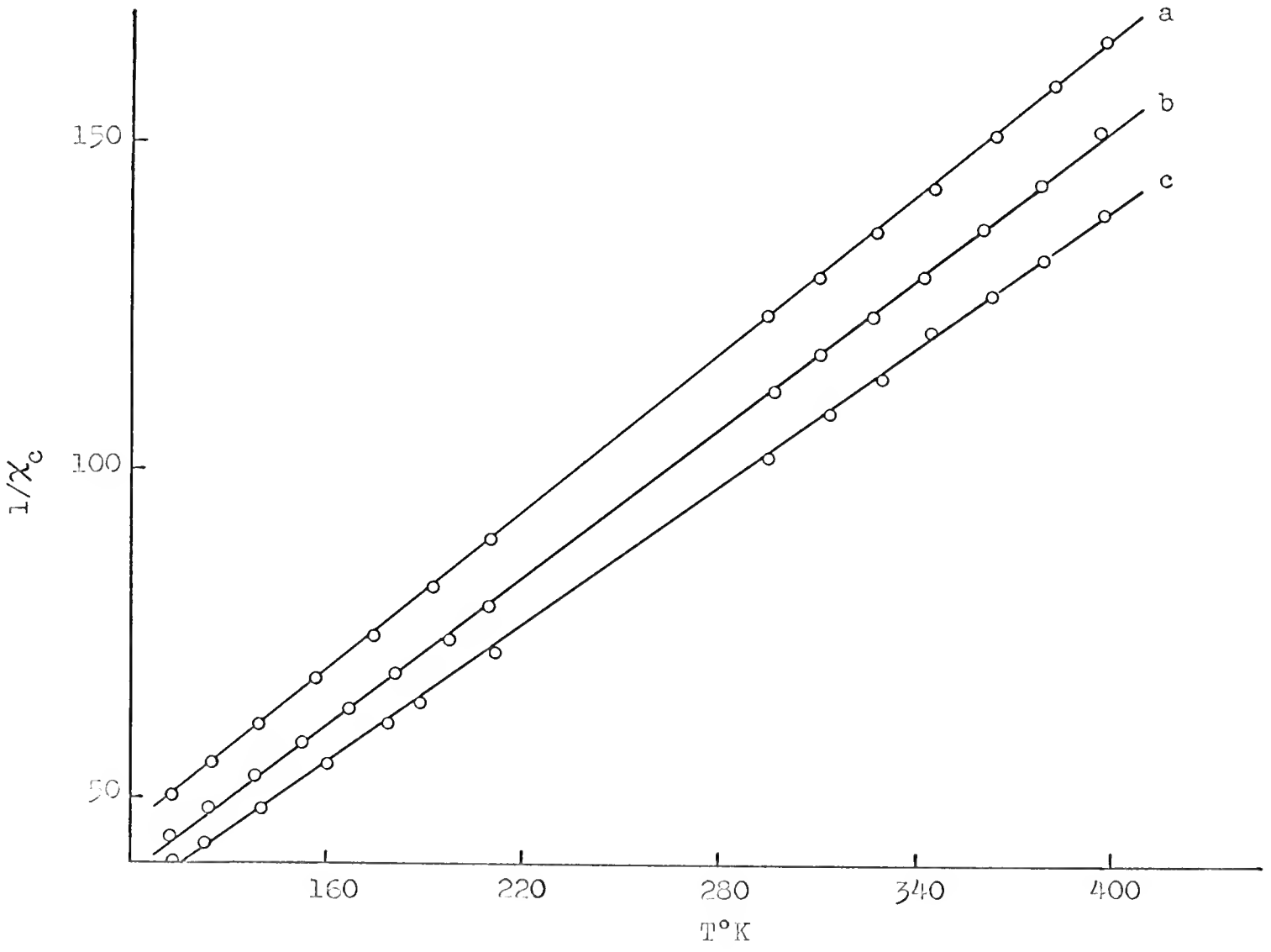

Fig. 17.-Temperature dependent susceptibility of (a) $[Co(NO_2)_2(PAPI)]$, (b) $[Co(NCS)_2(PAPI)]$, and (c) $[CoCl_2(PAPI)]$.

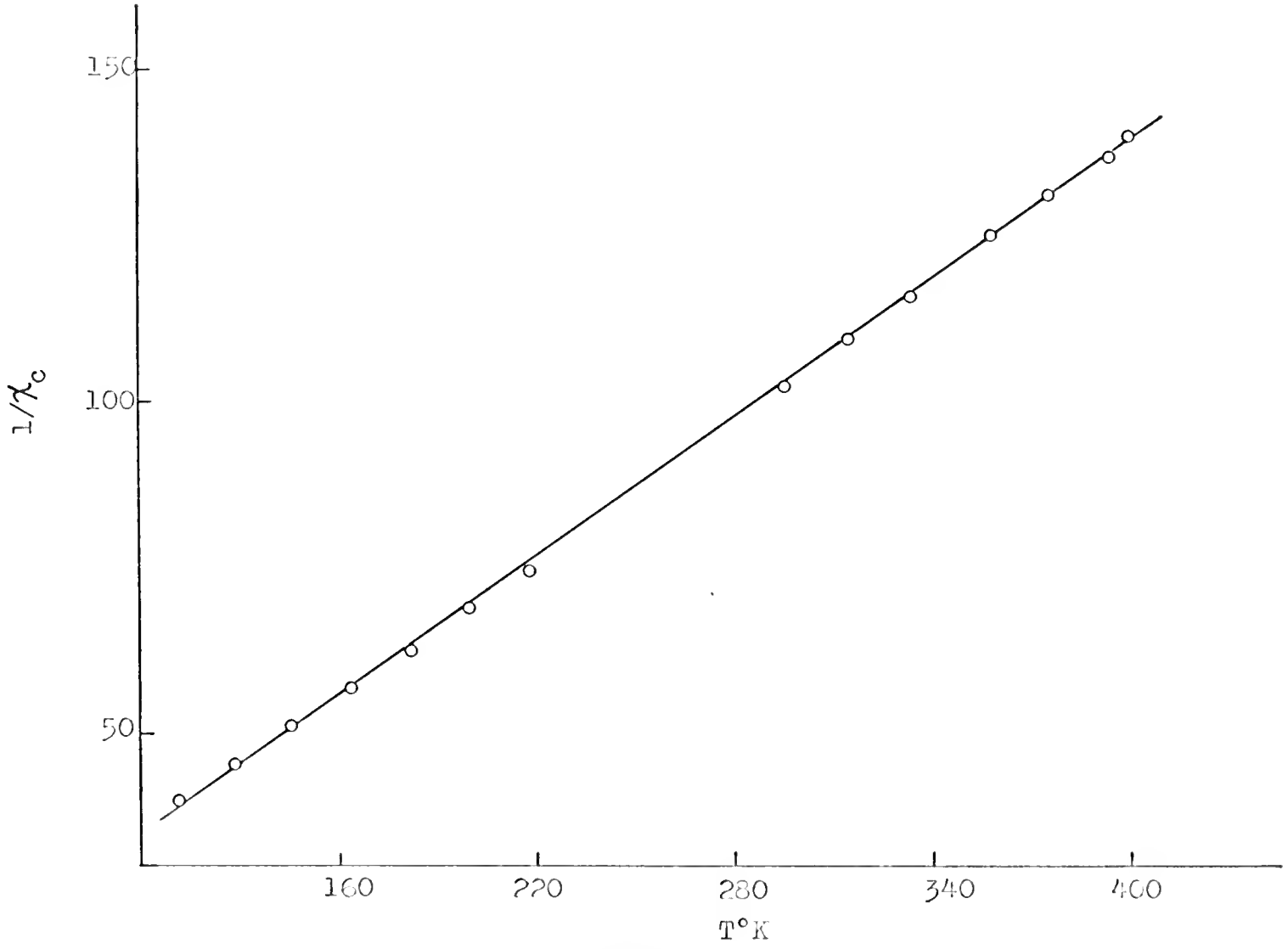

Fig. 18.-Temperature dependent susceptibility of [$CoBr_2$(PAPI)].

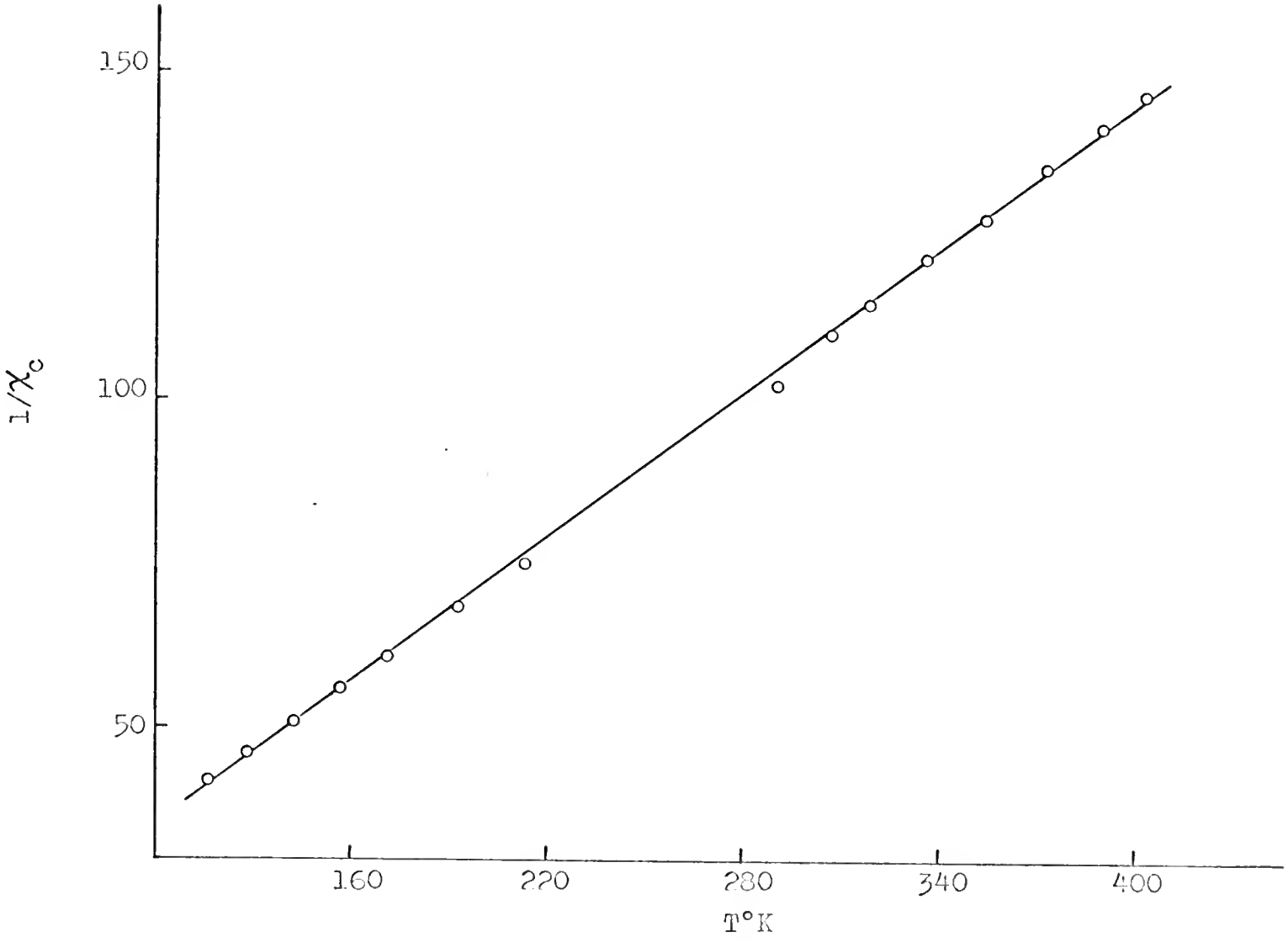

Fig. 19.-Temperature dependent susceptibility of $[CoI_2(PAPI)]$.

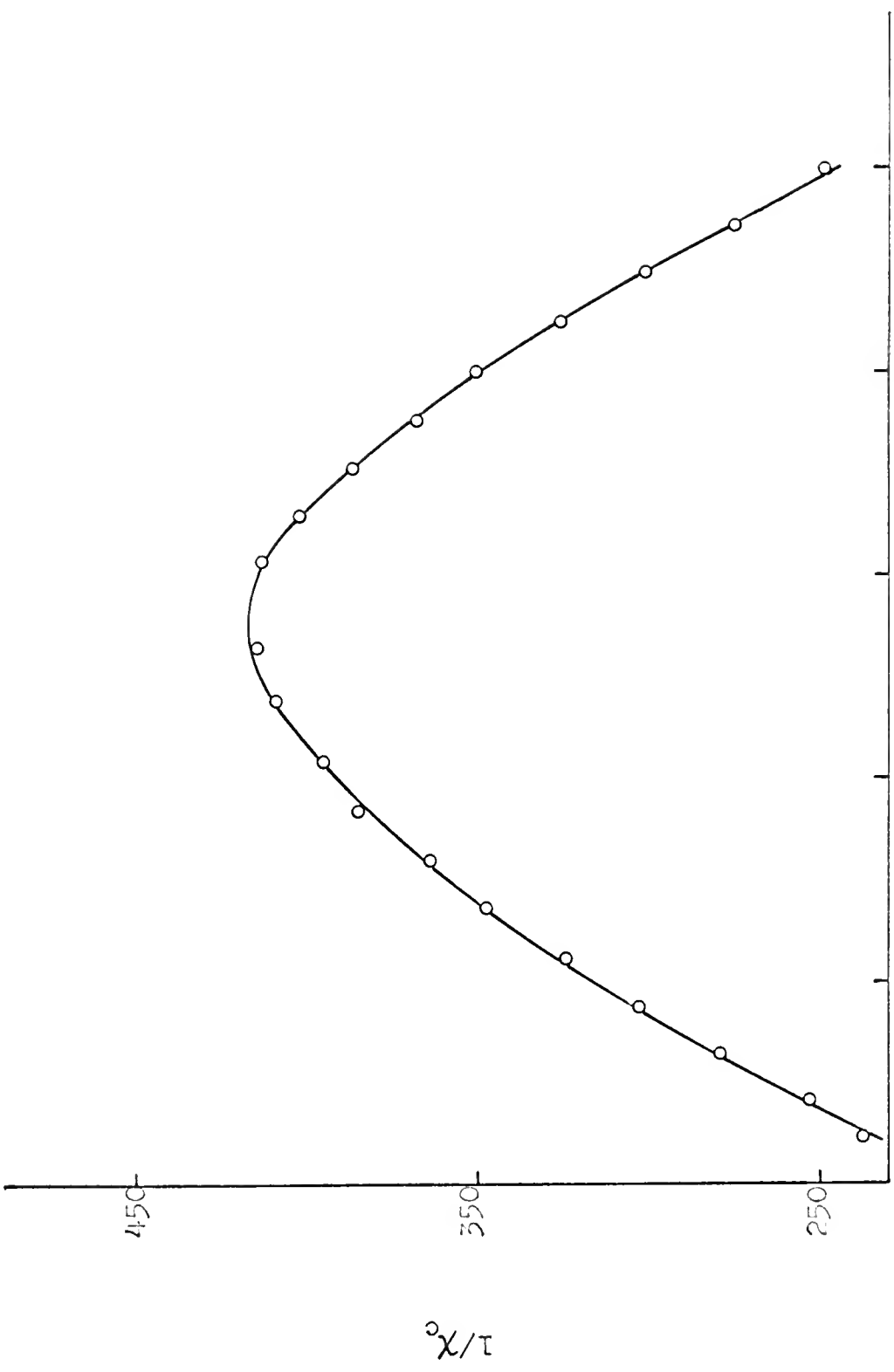

Fig. 20.-Temperature dependent susceptibility of $[Co((ClO_4)_2(PAP1)]$.

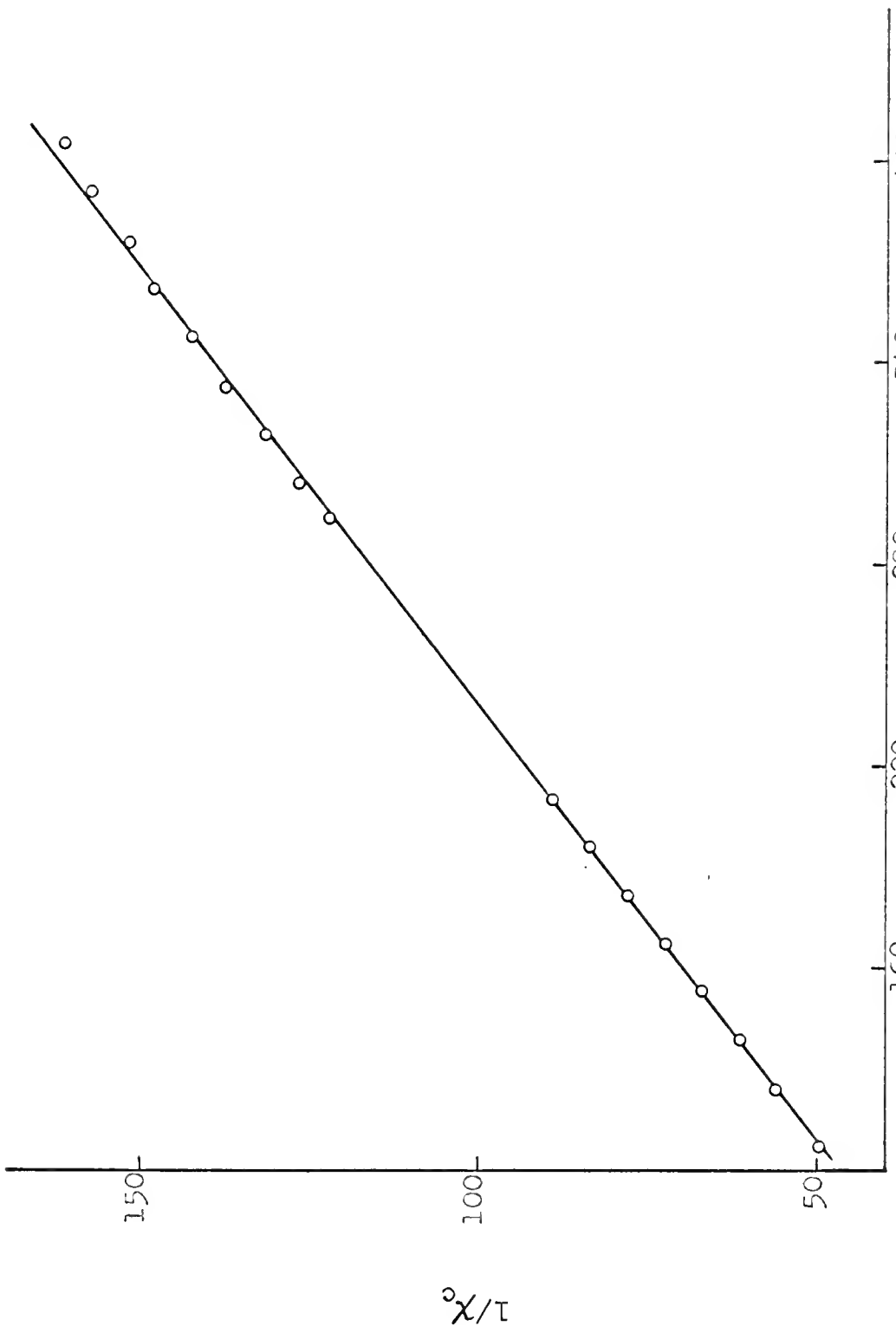

Fig. 21.-Temperature dependent susceptibility of green $CoBr_2(PAPI)$.

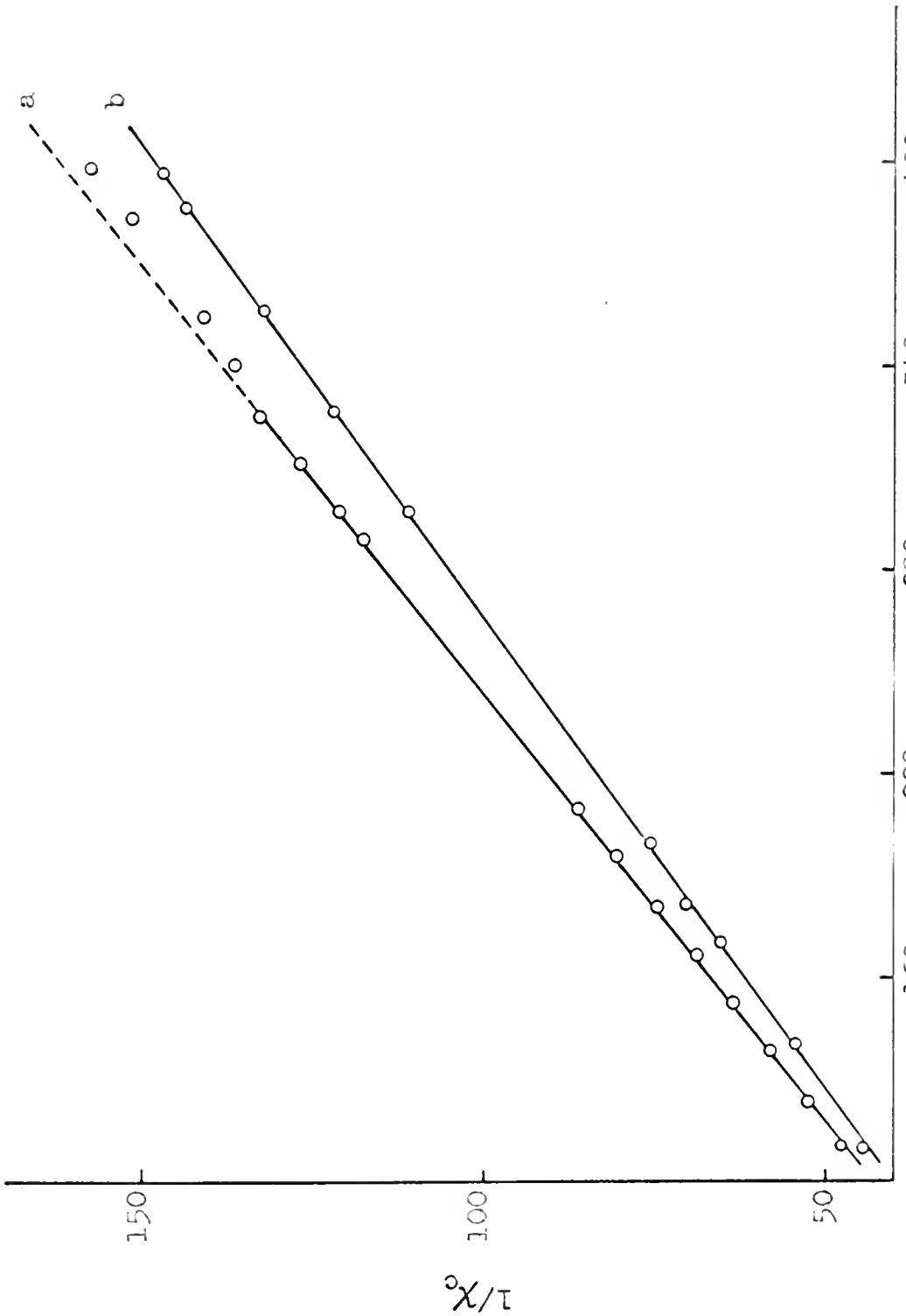

Fig. 22.-Temperature dependent susceptibility of (a) $[CoBr_2(PAT)_2]$ and (b) $[CoCl_2(PAT)_2]$.

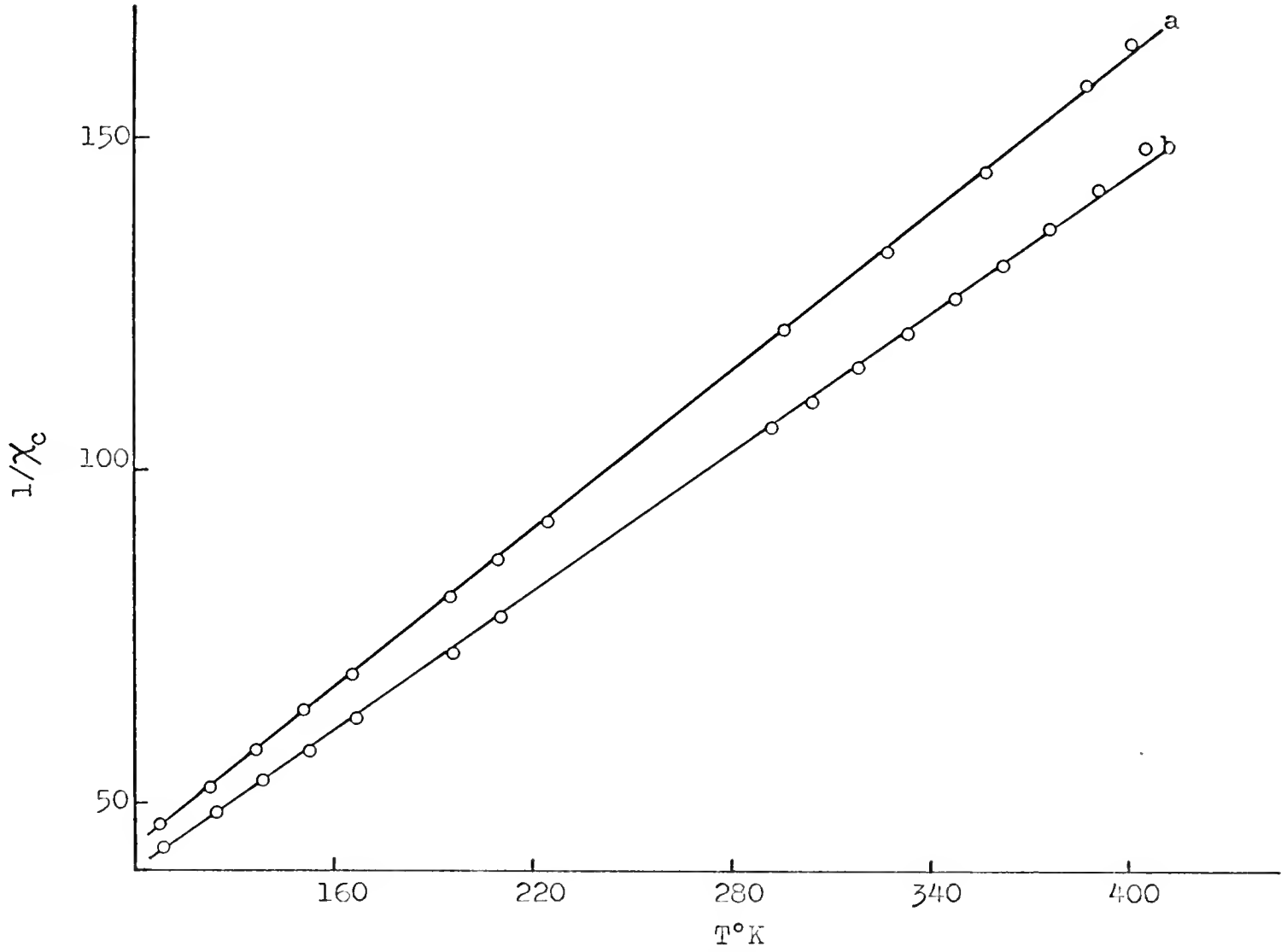

Fig. 23.-Temperature dependent susceptibility of (a) $[Co(NO_2)_2(PAT)_2]$ and (b) $[CoI_2(PAT)_2]$.

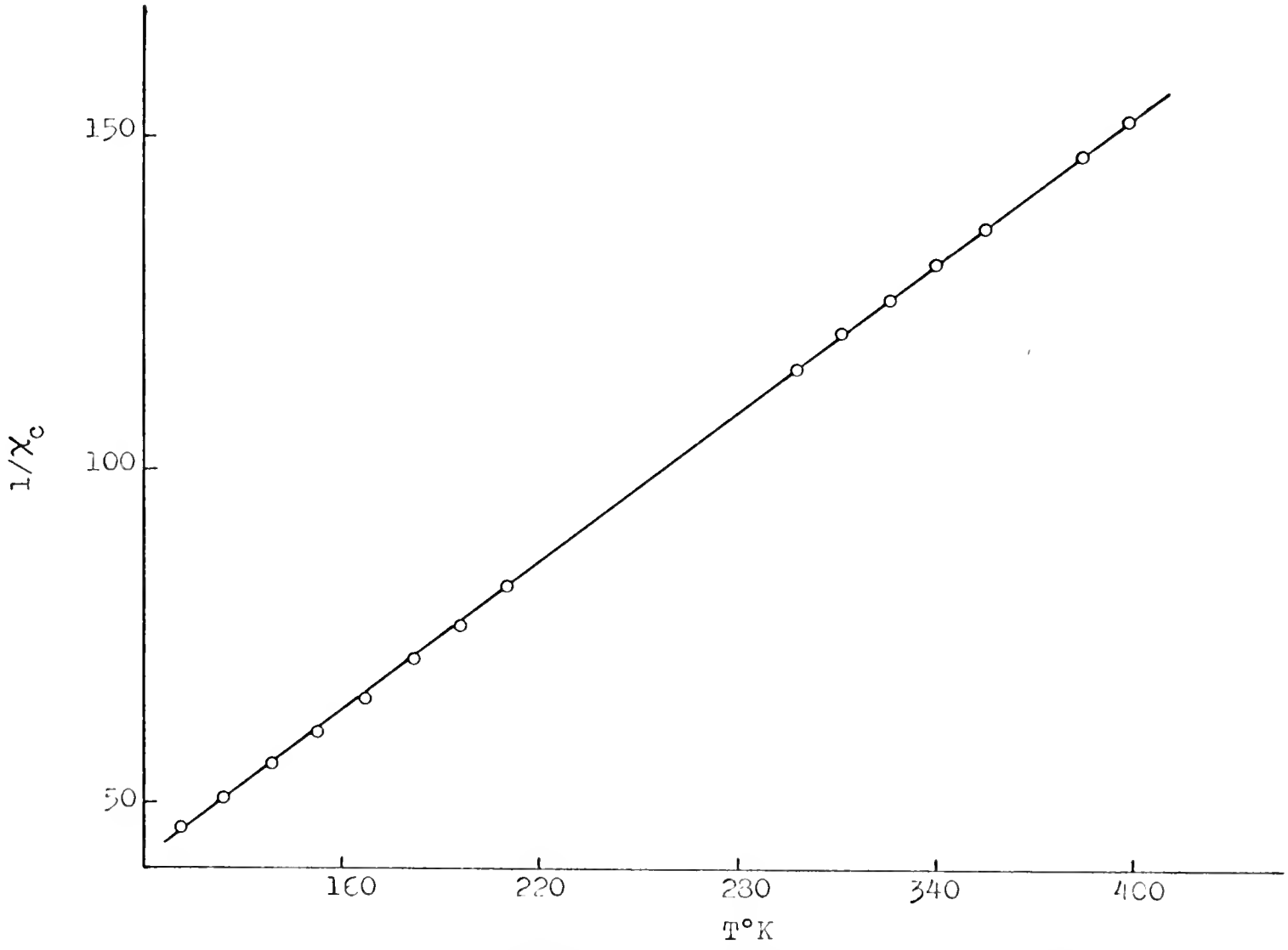

Fig. 24.-Temperature dependent susceptibility of $[Co(NCS)_2(PAT)_2]$.

TABLE 21

MAGNETIC MOMENTS OF COBALT(II) COMPLEXES AT 298°K AND CURIE AND WEISS CONSTANTS

Complex	μ_{eff}[a]	μ_{eff}[b]	μ_o	C	θ(°K)
$[CoCl_2(PAPI)]$	4.84	4.84	4.81	2.87	0
$[CoBr_2(PAPI)]$	4.84	4.83	4.81	2.87	0
$[CoI_2(PAPI)]$	4.75	4.75	4.71	2.75	3
$[Co(NO_2)_2(PAPI)]$	4.39	4.38	4.50	2.51	-15
$[Co(NCS)_2(PAPI)]$	4.62	4.62	4.63	2.66	- 2
$[Co(ClO_4)_2(PAPI)]$	2.45	2.45	----	----	Anomalous
$CoCl_2$(PAPI) green	4.54*	4.54*	4.69*	2.69*	-17*
$CoBr_2$(PAPI) green	4.40	4.39	4.56	2.58	-19
$[CoCl_2(PAT)_2]$	4.64	4.65	4.73	2.77	-11
$[CoBr_2(PAT)_2]$	4.44	4.44	4.49	2.50	- 8
$[CoI_2(PAT)_2]$	4.71	4.71	4.81	2.87	-14
$[Co(NO_2)_2(PAT)_2]$	4.44	4.44	4.51	2.52	-10
$[Co(NCS)_2(PAT)_2]$	4.56	4.55	4.65	2.68	-11

[a]Field strength = 6860 Gauss.

[b]Field strength = 5750 Gauss.

*Value reported by Petrofsky (37).

$\mu_o = 2.84\ C^{1/2}$.

TABLE 22

MAGNETIC MOMENTS OF NICKEL(II) COMPLEXES

Complex	Temperature, ^{o}K	μ_{eff}[a]	μ_{eff}[b]
$[NiCl_2(PAPI)]\cdot 3/2H_2O$	298.74	3.11	3.11
$[NiBr_2(PAPI)]\cdot 3/2H_2O$	297.52	3.25	3.25
$[NiI_2(PAPI)]$	297.37	3.06	3.06
$[Ni(H_2O)(PA)(PAPI)]$	298.74	2.96	2.96

[a]Field strength = 6860 Gauss.

[b]Field strength = 5750 Gauss.

As mentioned previously, high-spin cobalt(II) in an octahedral field has a $^4T_{1g}$ ground state. This triply degenerate state provides an orbital angular momentum contribution to the magnetic moment which increases the moment from 3.87 B.M. (spin-only value) to 4.1 B.M. The still larger values observed for high-spin octahedral complexes are explained on the basis of spin-orbit coupling which mixes in with the ground state some of the higher levels having orbital angular momentum.

Within a series of similar complexes, two factors should determine trends in the magnetic moments of these complexes. One factor is a variation in symmetry caused by the distortions within the series. The other factor is the variation in the energy separation between the ground state and the higher interacting levels. As the energy separation increases, the degree of mixing decreases.

High-spin complexes with a lower symmetry than O_h are expected to exhibit magnetic moments which are somewhat smaller than those with the O_h symmetry because a reduction in symmetry lifts the degeneracy of the ground state. The extent of distortion within a complex is expected to determine the degree of quenching of the orbital angular momentum contribution. On this basis, the observed magnetic moments were expected to reflect trends which would give some indication of the distortion within the series of

complexes; however, perusal of Tables 7 and 8 reveals that no such trend is apparent within the series of complexes investigated.

The isothiocyanato complex is probably the one which is most nearly octahedral of those within the series because the effective basicity of this group is closer to that of PAPI than is the basicity of any other one of the anions. In spite of this fact, the moments of the isothiocyanato complexes are among the lowest observed. Rather, a comparison of the Δ values of these complexes with their magnetic moments (Table 23) reveals that the energy separation between the ground state and the higher interacting levels is more important in determining the contribution of orbital angular momentum to the magnetic moment. The level being mixed in with the ground state is not necessarily the next higher level. However, this interacting level does depend inversely on the Δ values which were obtained spectroscopically (exception[$Co(NO_2)_2$(PAPI)]). Therefore, in conclusion, it may be stated that for the series of complexes investigated the magnetic moments are more sensitive to ligand field variations than to a reduction of the symmetry of the ground state.

The temperature dependent susceptibilities of the above complexes exhibit normal Curie or Curie-Weiss dependence. Within a series of similar complexes (except for

TABLE 23

SUMMARY OF Δ VALUES AND ROOM TEMPERATURE MAGNETIC MOMENTS

Complex	Δ, cm^{-1}	μ_{eff}
$[CoBr_2(PAT)_2]$	12,600	4.44
$[Co(NO_2)_2(PAT)_2]$	12,900	4.44
$[Co(NCS)_2(PAT)_2]$	11,800	4.56
$[CoCl_2(PAT)_2]$	11,900	4,64
$[CoI_2(PAT)_2]$	10,900	4.71
$[Co(NO_2)_2(PAPI)]$	9,800	4.39
$[Co(NCS)_2(PAPI)]$	12,000	4.62
$[CoI_2(PAPI)]$	11,200	4.75
$[CoBr_2(PAPI)]$	10,100	4.84
$[CoCl_2(PAPI)]$	9,800	4.84

$[Co(NO_2)_2(PAPI)]$, the Weiss constants are essentially the same. The curvature in the plot of $1/\chi_c$ vs T for $[CoBr_2(PAT)_2]$ (Figure 22) is due to the loss in weight of the sample at higher temperatures (see Electronic Spectra).

The validity of the prediction of eventual spin-pairing as a consequence of a tetragonal distortion was demonstrated with the $[Co(ClO_4)_2(PAPI)]$ complex. The room temperature magnetic moment (2.45 B.M.) could be interpreted as being characteristic of square planar cobalt(II) complexes (2.1-2.9 B.M.) (15). However, the infrared spectrum of this complex demonstrates that the perchlorate ions are indeed coordinated to the metal ion (see Vibrational Spectra). The magnetic susceptibility of a square planar complex would exhibit normal Curie-Weiss behavior; however, this complex exhibits anomalous behavior (Figure 20). In light of these observations, it is concluded that the complex is six-coordinate rather than square planar.

The anomalous behavior can be attributed to an equilibrium mixture of spin-states. The variation of the magnetic moment with temperature (Figure 25) is qualitatively in accordance with a change in the relative populations of the high- and low-spin states as described by a Boltzmann distribution over these states,

$$N_h/N_l = Ae^{-\Delta E/kT} \quad ,$$

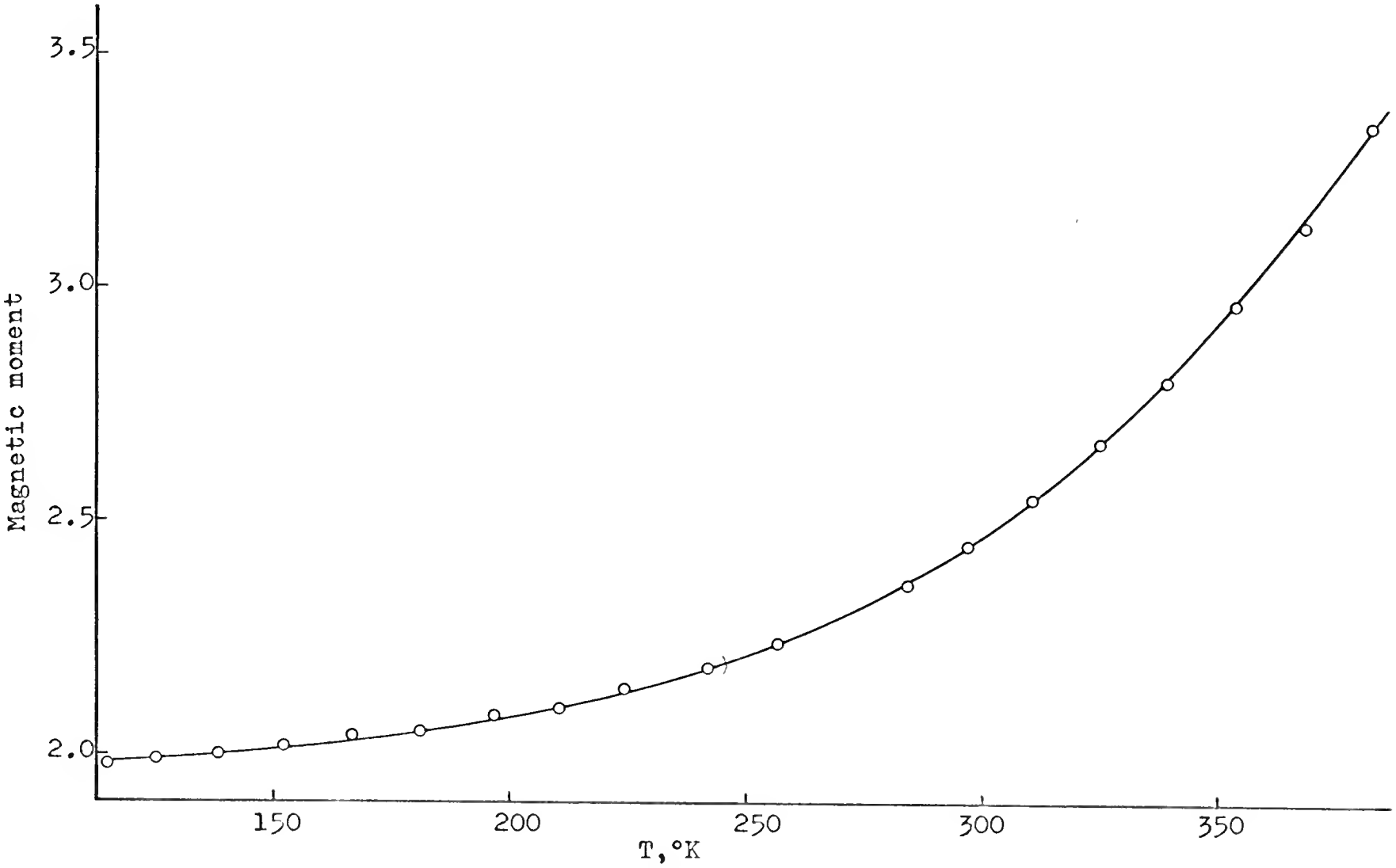

Fig. 25.-Temperature dependent magnetic moment of $[Co(ClO_4)_2(PAPI)]$.

where N_h and N_l are the populations of the high- and low-spin states, respectively; ΔE is the separation between these two states, and A is a proportionality constant.

The decrease in the magnetic moment with decreasing temperature depends upon two factors (see Formula): a lower temperature increases the population of the low-spin state and a lower temperature also decreases the internuclear separation between the metal and the ligand which in turn increases the separation, ΔE, between the two states provided the low-spin form is of lower energy.

In view of these observations, it is well established that a tetragonal distortion does eventually induce spin-pairing. However, it should be stated that since the perchlorate ion is such a weak ligand, a very large distortion is necessary before spin-pairing occurs within the series of complexes containing PAPI as the in-plane ligand. By using ligands which produce stronger in-plane ligand fields, however, such a large distortion may not be necessary. An investigation in this area (together with precise X-ray measurements) is a necessary extension of this investigation before subtle variations within a series of distorted complexes can be explained completely.

The magnetic moments of the two green PAPI complexes fall within the range characteristic of both octahedral (4.3-5.2 B.M.) and tetrahedral (4.3-5.1 B.M.) (23) cobalt(II)

complexes. However, principally because of the strong evidence indicative of tetrahedral complexes exhibited by the visible spectra (see Electronic Spectra) of these complexes, it has been concluded that these complexes are tetrahedral. The magnetic susceptibilities of these two complexes follow a Curie-Weiss relationship. The lower magnetic moment exhibited by the bromo complex (Table 21) appears to be due to a greater loss in symmetry which splits the higher interacting states which are contributing orbital angular momentum to the ground state. This variation in the moment between the two complexes is again an indication that at least one of the halide ions is coordinated to the metal.

The magnetic moments of each of the nickel(II) complexes fall in the range expected for high-spin, six-coordinate complexes. The variation in the magnetic moments is inversely dependent upon the Δ values exhibited by these complexes (the magnetic moment of the chloro complex being somewhat out of line). This behavior is again an indication that the energy separation between the ground state and higher interacting levels is more important in determining the amount of quenching of orbital angular momentum than is a slight reduction of the symmetry of the ground state.

X-ray diffraction patterns

An x-ray diffraction powder pattern of each complex was obtained in order to further characterize the complexes. The d-spacings and relative line intensities were determined and are tabulated in Appendix III.

The diffraction patterns of complexes within a series are similar; but, it can not be established unequivocally that the complexes are isomorphous with each other. The diffraction patterns of both the green $CoCl_2$(PAPI) and the green $CoBr_2$(PAPI) complexes are very distinct from those of the other PAPI complexes, that is, they exhibit only one very broad peak. This behavior is indicative of amorphous solids and it may even suggest polymeric complexes.

This large difference in the x-ray patterns of the two types of PAPI complexes was a result of a small variation in their preparations (see Experimental Procedures). The method of preparation for the octahedral PAPI complexes is another example of the growing number of template reactions in which a metal ion serves to promote the synthesis of ligands which are difficult to prepare otherwise.

The change in the diffraction patterns of the unheated and heated [$CoBr_2(PAT)_2$] complexes demonstrates that definite rearrangements have occurred in the solid upon heating the complex above 66°C (see Electronic Spectra).

SUMMARY

The synthesis and characterization of sixteen new complexes of cobalt(II) and nickel(II) are reported. These complexes are of the type MX_2L_2 or MX_2L' where L refers to 2-pyridinal-p-tolylimine and L' refers to bis(2-pyridinal)-o-phenylenediimine and X may be Cl^-, Br^-, I^-, NO_2^-, or ClO_4^-. The diffuse reflectance spectrum of each complex was determined between 3,000 A and 13,500 A. Assignments were made for some of the transitions and Δ values were evaluated from specific absorptions.

The magnetic susceptibilities of the complexes were determined at room temperature. Twelve of them were determined as a function of temperature. Eleven of these complexes exhibit normal Curie-Weiss behavior. One cobalt(II) complex, the diperchlorato complex, exhibits anomalous magnetic behavior which is interpreted in terms of an equilibrium mixture of spin-states (quartet-doublet). These observations demonstrate that spin-pairing does occur as a consequence of an axial distortion of a six-coordinate d^7 ion; moreover, one may infer that a rather large distortion is necessary when the in-plane field is provided by nitrogen atoms either of the heterocyclic aromatic amine or

of the imine type or of both types. Thus, it is concluded that the equilibrium mixture of spin-states characterizing a number of six-coordinate cobalt(II) complexes in which all six coordination positions are occupied by nitrogen atoms of this type is not attributable to a slight tetragonal distortion.

APPENDICES

APPENDIX I

TABLE 24

INFRARED ABSORPTION BANDS (CM^{-1}) FOR COBALT(II)--PAT COMPLEXES

Assignment	PAT	$[CoCl_2(PAT)_2]$	$[CoBr_2(PAT)_2]$	$[CoI_2(PAT)_2]$	$[Co(NO_2)_2(PAT)_2]$	$[Co(NCS)_2(PAT)_2]$
H_2O	3460 m(b)	3500 s(b)	3510 s(b)	3500 w(b)	3500 w(b)	3500 m(b)
S+ CH	2976 w	3040 w	3070 m	----	3070 w	3000 w(b)
	2907 w	2960 (sh)	2940 w	----	2950 w	----
S+ C≡N	----	----	----	----	----	2090 vs
S+ C=N (Acyclic)	1626 s	1630 m	1630 m	1620 (sh)	1620 m	1630 w
Band I (py ring)	1582 s	1590 s	1590 s	1590 s	1590 s	1590 s
	1543 (sh)	1540 m	----	----	----	----
Band II (py ring)	1567 s	1560 m	1560 m	1560 m	1560 m	1560
Benzene (ring)	1506 s	1505 s	1510 s	1500 s	1505 s	1500 m
Band III (py ring)	1462 s	1480 s	1480 m	1470 m	1475 m	1470 w

TABLE 24 - Continued

Assignment	PAT	$[CoCl_2(PAT)_2]$	$[CoBr_2(PAT)_2]$	$[CoI_2(PAT)_2]$	$[Co(NO_2)_2(PAT)_2]$	$[Co(NCS)_2(PAT)_2]$
Band IV (py ring)	1435 s	1440 s	1440 s	1440 s	1440 (sh)	1440 m
S+ ONO (assym.)	----	----	----	----	1408 s	----
S+ C-N (tolyl-N)	1348 m	1360 s	1360 s	1360 s	1360 m	1360 m
	1292 w	1310 s	1310 s	1310 s	1305 m	1300 m
	1289 w	1265 m	1265 m	1260 m	1265 m	1260 m
d CH or py ring vib.	1233 w	1235 m	1235 m	1235 m	1235 m	1230 (sh)
p-Substitution (tolyl)	1214 w	1215 m	1215 (sh)	1210 (sh)	1210 (sh)	1210 (sh)
	1198 m	1195 s	1195 s	1190 s	1195 m	1195 m
	----	1160 s	1160 s	1155 s	1155 s	1155 m
p-Substitution (tolyl)	1088 w	1110 m	1110 m	1110 s	1110 s	1100 m
S+ ONO (symm.)	----	----	----	----	1070 s	----
	----	1045 m	1045 m	1050 s	1050 s	1040 m
d CH or py ring vib.	1018 w	1020 s	1020 s	1015 s	1015 s	1020 s
	----	985 m	990 w	995 w	990 (sh)	990 w
	----	973 m	965 w	965 w	975 w	960 w
	----	940 w	940 w	942 w	940 m	935 (sh)
	----	912 s	910 s	910 s	912 s	910 s
	----	852 w	880 w	----	----	----
	----	842	----	844 (sh)	840 (sh)	840 (sh)
	----	828 (sh)	----	836 s	830 (sh)	----

TABLE 24 - Continued

Assignment	PAT	$[CoCl_2(PAT)_2]$	$[CoBr_2(PAT)_2]$	$[CoI_2(PAT)_2]$	$[Co(NO_2)_2(PAT)_2]$	$[Co(NCS)_2(PAT)_2]$
d CH (tolyl ring)	823 vs 779 s	818 s 780 s	820 s 778 s	823 s 789 s	818 s 782 s	820 s 780 (sh)
d CH (py ring)	769 s	770 (sh)	----	772 s	774 s	772 s
d CH (py ring)	737 s	749 m	747 m	742 s	748 m	746 m
d CH (toly-ring)	704 w(b)	710 m	710 m	705 m	708 m	710 m

TABLE 25

INFRARED ABSORPTION BANDS (CM^{-1}) FOR COBALT(II)--PAPI COMPLEXES

Assignment	$[CoCl_2(PAPI)]$	$[CoBr_2(PAPI)]$	$[CoI_2(PAPI)]$	$[Co(NO_2)_2(PAPI)]$
H_2O	----	----	----	3470 w (b)
	3200 m(b)	----	----	----
S+ CH	3060 w	3050 m(b)	3060 w(vb)	3050 w(b)
S+ C=N (Acyclic)	1620 m	1620 m	1615 m	1620 s
Band I (py ring)	1590 s	1590 s	1590 s	1590 s
Band II (py ring)	1560 w	1560 w	1560 (sh)	1565 w
	1490 m	1485 m	1485 m	1490 s
Band III (py ring)	1460 w	1465 w	1465 m	1465 (sh)
Band IV (py ring)	1440 m	1445 m	1445 m	1450 m
S+ C-N (phenyl-N)	1370 s	1365 s	1365 s	1370 s
	1300 m	1300 m	1295 m	1300 s
	1265 m	1265 m	1260 m	1265 m
d CH or py ring vib.	1230 m	1230 m	1230 m	1230 sh
	1205 m	1205 m	1205 m	1205 s
	1155 m	1158 m	1158 m	----

TABLE 25 - Continued

Assignment	$[CoCl_2(PAPI)]$	$[CoBr_2(PAPI)]$	$[CoI_2(PAPI)]$	$[Co(NO_2)_2(PAPI)]$
S+ ONO	----	----	----	1135 s
(symm.)	1155 m	1158	1158	----
	1110 m	1110 m	1110 m	1100 (sh)
	1045 m	1025 w	1025 w	1025 m
d CH or	1015 s	1015 (sh)	1015 m	1010 s
py ring vib.	----	----	1010 s	----
	980 w	980 m	978 m	980 (sh)
	960 m	957 m	----	----
	950 m	----	950 s	950 s
	----	942 w	940 w	----
	906 m	905 m	905 m	905 s
	815 w	----	----	----
d ONO	----	----	----	845 m
	----	----	----	812 s
	785 s	784 s	786 (sh)	780 (sh)
	----	----	780 s	----
d CH	762 s	761 s	760 s	767 (vs)
(py ring)				
d CH	746 s	746 s	745 s	745 s
(py ring)	684 w	686 w	685 m	680 w

TABLE 25 - Continued

Assignment	$[Co(NCS)_2(PAPI)]$	$[Co(ClO_4)_2(PAPI)]$	$CoCl_2(PAPI)$ green	$CoBr_2(PAPI)$ green
H_2O	3500 m(b)	3500 w(b)	3500 s(b)	3500 m(b)
S+ CH	3090 m	3050 w(b)	3100 m	3100 m
S+ C≡N	2090 vs	----	----	----
S+ C=N (Acyclic)	1620 m	1620 w	----	----
Band I (py ring)	1590 s	1595 s	1600 s	1600 s
Band II (py ring)	1560 w 1485 m	1555 w 1480 s	1570 w 1480 s	1570 w 1480 s
Band III (py ring)	----	1460 m	----	----
Band IV (py ring)	1440 m	1440 m	1430 s	1430 s
S+ C-N (phenyl-N)	1365 s ---- 1300 m ---- 1265 m ----	1360 m ---- 1310 m ---- 1265 m ----	---- 1330 w 1320 w 2195 m ---- 2145 w	---- 1330 w 1320 w 1295 m ---- 1250 w
d CH or py ring vib.	1225 m 1200 m	1220 w 1205 m	---- 1210	---- 1210

TABLE 25 - Continued

Assignment	$[Co(NCS)_2(PAPI)]$	$[Co(ClO_4)_2(PAPI)]$	$CoCl_2(PAPI)$ green	$CoBr_2(PAPI)$ green
	1155 m	1163 s	1155 m	1155 m
ClO_4 $\nu_3(E)$	----	1110 vs(b)	----	----
	----	----	1110 w	1110 w
ClO_4 $\nu_3(A_1)$	----	1035 vs(b)	----	----
	----	----	1050 m	1055 m
	1025 w	----	1020 m	1020 m
d CH or	1010 s	----	----	----
py ring vib.	972 w	----	980 w	----
	945 m	----	940 w	940 w
ClO_4 $\nu_1(A_1)$	----	920 m	----	----
	----	----	920 w	920 w
	902	----	----	----
	----	----	862 w	862 w
	----	----	828 w	828 w
	815 w	----	812 w	812 w
S-H C-S	800 w	----	----	----
	780 (sh)	----	790 m	788 (sh)
	774 s	772 vs	----	----
d CH	762 s	----	764 (sh)	762 (sh)
(py ring)				
d CH	745 s	742 m	746 s(b)	746 s(b)
(py ring)	685 w	----	692 w	692 w

TABLE 26

INFRARED ABSORPTION BANDS (CM^{-1}) FOR NICKEL(II)--PAPI COMPLEXES

Assignment	$[NiCl_2(PAPI)]$	$[NiBr_2(PAPI)]$	$[NiI_2(PAPI)]$	$[Ni(H_2O)(PA)](ClO_4)_2$
H_2O	3420 s(b) 3200 s(b)	3410 s(b) 3250 s(b)	3500 w(b) 3280 s(b)	3500 s 3280 s
S+ CH	----	----	3040 w	3100 w
S+ C=O	---- ----	---- ----	---- ----	1710 m 1650 s
S+ C=N (Acyclic)	1620 m	1620 m	1620 m	1620 w
Band I (py ring)	1600 s	1600 s	1595 s	1600 s
Band II (py ring)	1565 (sh) 1485 s	1560 w 1480 m	1565 (sh) 1480 m	1565 w 1485 m
Band III (py ring)	1460 s	1460 m	1460 w	1465 m
Band IV (py ring)	1435 s	1435 m	1435 w	1425 (sh)
S+ C-N (phenyl-N)	1365 s 1300 s 1260 m 1215 s 1205 m	1360 m 1300 m 1260 m 1220 m 1200 m	1360 m 1305 m 1260 m 1220 m 1200 m	1365 m 1305 m 1265 m 1220 (sh) 1210 s

TABLE 26 - Continued

Assignment	$[NiCl_2(PAPI)]$	$[NiBr_2(PAPI)]$	$[NiI_2(PAPI)]$	$[Ni(H_2O)(PA)](ClO_4)_2$
	1175 m	1175 w	1165 (sh)	1160 (sh)
	1155 m	1150 m	1155 s	-----
	1115 s	1115 s	-----	-----
	1105 (sh)	1105 m	1100 s	-----
	1075 s	1075 s	-----	-----
	1045 m	1040 m	1050 m	-----
ClO_4^- $\nu_3(F_2)$	-----	-----	-----	1085 vs (vb)
d CH or	1015 s	1010 s	1015 s	1020 (sh)
py ring vib.	970 m	970 (sh)	970 m	967 w
	942 s	940 s	945 m	945 m
ClO_4^- $\nu_1(A_1)$	-----	-----	-----	930 (sh)
	905 s	905 m	900 m	906 w
	848 s	845 m	-----	860 m
	772 vs	775 vs	770 vs	776 s
d CH	760 (sh)	760 (sh)	760 s	760 (sh)
(py ring)	742 s	742 s	740 s	742 m
	682 s	680 m	682 m	682 m

APPENDIX II

TABLE 27

MOLAR SUSCEPTIBILITIES OF LIGANDS AND ANIONS

Ligand or anion	$\lambda_m \times 10^6$
2-Pyridinal-p-tolylimine (43)	- 61
bis(2-pyridinal)-o-phenylenediimine (42)	-153
2-Pyridine-carboxaldehyde (42)	- 56
Chloride (42)	- 26
Bromide (42)	- 36
Iodide (42)	- 52
Nitrite (42)	- 10
Perchlorate (43)	- 30
Thiocyanate (42)	- 35
Water (42)	- 13

APPENDIX III

TABLE 28

d-SPACINGS AND RELATIVE LINE INTENSITIES

Complex	d-Spacing (in angstroms)	Relative intensity
$[CoCl_2(PAPI)]$	9.4	0.88
	8.8	0.36
	6.8	1.00
	5.4	0.61
	4.8	0.58
	4.6	0.49
	3.4	0.84
	3.2	0.28
	3.2	0.26
$[CoBr_2(PAPI)]$	9.6	0.44
	8.8	0.21
	6.6	0.37
	6.4	0.23
	5.8	0.36
	5.4	0.26
	4.9	0.42
	4.3	0.18
	4.2	0.45
	4.1	0.23
	3.8	0.21
	3.7	0.18
	3.5	0.18
	3.3	1.00
	2.8	0.14
	2.7	0.20
	2.6	0.15
$[CoI_2(PAPI)]$	9.8	0.71
	6.7	0.84
	6.1	0.77
	5.5	0.41
	4.9	0.91
	4.3	0.57
	4.2	0.65
	3.9	1.00

TABLE 28 - Continued

Complex	d-Spacing (in angstroms)	Relative intensity
$[NiCl_2(PAPI)]\cdot 3/2\ H_2O$	9.6	0.48
	9.2	1.00
	7.2	0.57
	6.8	0.17
	6.2	0.32
	5.5	0.20
	5.1	0.14
	4.6	0.23
	4.6	0.26
	4.4	0.22
	4.1	0.13
	3.7	0.57
	3.5	0.17
	3.3	0.14
	3.0	0.18
	2.8	0.12
$[NiBr_2(PAPI)]\cdot 3/2\ H_2O$	9.6	0.80
	9.0	0.84
	7.4	0.56
	7.2	0.58
	4.6	0.45
	4.3	0.48
	3.8	0.48
	3.7	1.00
	3.0	0.26
	2.8	0.34
	2.6	0.27
$[NiI_2(PAPI)]$	9.6	0.51
	7.9	0.36
	5.4	0.48
	4.9	0.45
	4.5	0.51
	3.7	0.44
	3.6	0.33
	3.2	0.67
	3.1	1.00
	2.9	0.19
	2.7	0.26
	2.6	0.26
$[Ni(H_2I)(PA)(PAPI)](ClO_4)_2$	9.0	0.78
	7.9	0.59
	6.4	0.47
	6.0	0.53
	5.5	0.67

TABLE 28 - Continued

Complex	d-Spacing (in angstroms)	Relative intensity
	4.8	0.56
	4.1	1.00
	3.9	0.85
	3.6	0.48
$[CoCl_2(PAT)_2]$	9.2	1.00
	7.4	0.31
	7.2	0.11
	5.9	0.15
	5.2	0.19
	4.5	0.13
	4.3	0.11
	3.9	0.12
	3.6	0.19
	3.5	0.15
	3.4	0.07
	3.2	0.06
	2.8	0.08
	2.7	0.09
$[CoBr_2(PAT)_2]$ (unheated)	10.5	1.00
	8.2	0.11
	7.0	0.08
	6.2	0.18
	5.9	0.24
	5.5	0.16
	4.2	0.12
	4.1	0.11
	3.9	0.11
	3.6	0.08
	3.2	0.10
	3.1	0.14
$[CoBr_2(PAT)_2]$ (heated)	8.1	0.52
	7.2	1.00
	7.1	0.49
	6.9	0.43
	6.8	0.29
	5.4	0.62
	5.0	0.23
	4.9	0.17
	4.6	0.21
	4.3	0.22
	4.2	0.33
	3.9	0.60
	3.7	0.10
	3.6	0.49

TABLE 28 - Continued

Complex	d-Spacing (in angstroms)	Relative intensity
	3.5	0.30
	3.4	0.80
	3.3	0.12
	3.2	0.25
	3.1	0.21
	3.1	0.43
	2.9	0.20
	2.8	0.14
	2.8	0.10
	2.6	0.14
	2.6	0.26
	2.6	0.36
$[CoI_2(PAT)_2]$	7.4	0.97
	6.0	0.89
	5.5	1.00
	5.2	0.71
	4.8	0.80
	4.5	0.63
	4.1	0.74
	3.7	0.60
	3.7	0.69
	3.6	0.86
	3.0	0.63
$[Co(NO_2)_2(PAT)_2]$	10.8	0.61
	8.8	0.55
	8.0	0.37
	7.1	0.19
	7.0	1.00
	5.4	0.32
	5.1	0.20
	4.9	0.12
	4.5	0.10
	4.3	0.26
	4.2	0.22
	3.9	0.41
	3.8	0.28
	3.6	0.15
	3.4	0.14
	3.1	0.17
	2.8	0.11

TABLE 28 - Continued

Complex	d-Spacing (in angstroms)	Relative intensity
$[Co(NCS)_2(PAT)_2]$	11.2	0.54
	8.9	0.44
	8.5	0.35
	7.1	0.29
	6.0	1.00
	5.6	0.60
	5.4	0.61
	5.0	0.24
	4.4	0.36
	4.3	0.80
	4.2	0.34
	3.9	0.80
	3.7	0.20
	3.6	0.13
	3.2	0.41
	3.1	0.17
	2.9	0.21

BIBLIOGRAPHY

1. G. Bahr and H. Thamlitz, A. anorg. allgem. Chem., 282, 3 (1955).

2. C. J. Ballhausen, "Introduction to Ligand Field Theory" (McGraw-Hill Book Company, Inc., New York, 1962). p. 255.

3. C. J. Ballhausen and C. K. Jorgensen, Acta Chem. Scand., 9, 116 (1955).

4. C. J. Ballhausen and A. D. Liehr, J. Am. Chem. Soc., 81, 538 (1959).

5. J. L. Burmeister and F. Basolo, Inorg. Chem., 3, 1587 (1964).

6. M. M. Chamberlain and J. C. Bailar, Jr., J. Am. Chem. Soc., 81, 6412 (1959).

7. J. Chatt and L. A. Duncanson, Nature, 178, 997 (1956).

8. E. A. Clevenger, "Thesis-1961." The University of Florida.

9. F. A. Cotton, O. D. Faut, D. M. L. Goodgame, and R. H. Holm, J. Am. Chem. Soc., 83, 1780 (1961).

10. F. A. Cotton, D. M. L. Goodgame, M. Goodgame, and A. Sacco, J. Am. Chem. Soc., 83, 1780 (1961).

11. F. A. Cotton and M. Goodgame, J. Am. Chem. Soc., 83, 1777 (1961).

12. F. A. Cotton and R. H. Holm, J. Am. Chem. Soc., 82, 2983 (1960).

13. N. F. Curtis, J. Chem. Soc., 3147 (1961).

14. R. E. Figgins and D. H. Busch, J. Am. Chem. Soc., 82, 822 (1960).

15. B. N. Figgis and R. S. Nyholm, J. Chem. Soc., 12 (1954).

16. B. N. Figgis and R. S. Nyholm, J. Chem. Soc., 331 (1959).

17. H. M. Fisher and R. C. Stoufer. In press.

18. D. M. L. Goodgame and L. M. Venanzi, J. Chem. Soc., 616 (1963).

19. M. Goodgame and F. A. Cotton, J. Am. Chem. Soc., 84, 1543 (1962).

20. J. S. Griffith, J. Inorg. Nucl. Chem., 2, 229 (1956).

21. B. J. Hathaway and A. E. Underhill, J. Chem. Soc., 3091 (1961).

22. R. H. Holm and F. A. Cotton, J. Chem. Phys., 31, 788 (1959).

23. R. H. Holm and F. A. Cotton, J. Chem. Phys., 32, 1168 (1960).

24. C. K. Jorgensen, "Absorption Spectra and Chemical Bonding in Complexes" (Addison-Wesley Publishing Company, Inc., Massachusetts, 1962). p. 109.

25. C. K. Jorgensen, Technical Report to the U. S. Army, Sept. 1958.

26. J. Lewis, R. S. Nyholm, and P. W. Smith, J. Chem. Soc., 4590 (1961).

27. J. Lewis and R. G. Wilkins, Eds., "Modern Coordination Chemistry" (Interscience Publishers, Inc., New York, 1960). p. 406.

28. A. D. Liehr, J. Phys. Chem., 67, 1314 (1963).

29. D. A. MacInnes, "The Principles of Electrochemistry" (Reinhold Publishing Corporation, New York, 1939). p. 359.

30. G. Maki, J. Chem. Phys., 28, 651 (1958).

31. G. Maki, J. Chem. Phys., 29, 162 (1959).

32. G. A. Melson and D. H. Busch, J. Am. Chem. Soc., 86, 4834 (1964).

33. K. Nakamoto, "Infrared Spectra of Inorganic and Coordination Compounds" (John Wiley and Sons, Inc., New York, 1963). pp. 155-175.

34. L. E. Orgel, Report to X Solvay Council, Brussels (1956).

35. L. E. Orgel, Quart. Revs., 8, 422 (1954).

36. S. F. Pavkovic and D. W. Meek, Inorg. Chem., 4, 20 (1965).

37. J. L. Petrofsky, "Thesis-1962." The University of Florida.

38. M. A. Robinson and D. H. Busch, Inorg. Chem., 2, 1171 (1963).

39. M. A. Robinson, J. D. Curry, and D. H. Busch, Inorg. Chem., 2, 1178 (1963).

40. A. Sabatini and I. Bertini, Inorg. Chem., 4, 959 (1965).

41. A. Sacco and F. A. Cotton, J. Am. Chem. Soc., 84, 2043 (1962).

42. P. W. Selwood, "Magnetochemistry" (Interscience Publishers, Inc., New York, 1956). pp. 91-97.

43. R. C. Stoufer, "Dissertation-1958." The Ohio State University.

44. R. C. Stoufer, W. B. Hadley, D. H. Busch, J. Am. Chem. Soc., 83, 3732 (1961).

45. R. C. Stoufer, D. W. Smith, E. A. Clevenger, and T. E. Norris. In press.

46. A. Turco and C. Pecile, Nature, 191, 66 (1961).

47. A. E. Wickenden and R. A. Krause. In press.

BIOGRAPHICAL SKETCH

Oscar Ramirez, Jr. was born July 3, 1940, in San Antonio, Texas. After attending Ogden Elementary School and Washington Irving Junior High School, he attended Brackenridge Senior High School and was graduated in May, 1958. In May, 1962, he received the degree of Bachelor of Science from Trinity University, San Antonio, Texas and at the same time was commissioned a second lieutenant in the United States Army.

While under extended leave from the Army, he began his graduate studies in September, 1962, at the University of Florida. From that time until June, 1963, he held a graduate assistantship and from July, 1963, through August, 1964, he held a research assistantship on a project supported by the National Science Foundation. From September, 1964, through August, 1965, he held a National Aeronautics and Space Administration Trainee Fellowship.

Mr. Ramirez is married to the former Patricia Ann Dersch. He is a member of Alpha Chi, Phi Kappa Phi, and the American Chemical Society.

This dissertation was prepared under the direction of the chairman of the candidate's supervisory committee and has been approved by all members of that committee. It was submitted to the Dean of the College of Arts and Sciences and to the Graduate Council, and was approved as partial fulfillment of the requirements for the degree of Doctor of Philosophy.

August 14, 1965

Ernest H. Cox
Dean, College of Arts and Sciences

Dean, Graduate School

Supervisory Committee:

R. Carl Stouffer
Chairman

R. D. Dresden